photonics

MDPI

Review

The Structure and Applications of Fused Tapered Fiber Optic Sensing: A Review

Siqi Ban [1] and Yudong Lian [1,2,3,4,*]

[1] Center for Advanced Laser Technology, Hebei University of Technology, Tianjin 300401, China; 213835@stu.hebut.edu.cn
[2] Hebei Key Laboratory of Advanced Laser Technology and Equipment, Tianjin 300401, China
[3] Tianjin Key Laboratory of Electronic Materials and Devices, Tianjin 300401, China
[4] State Key Laboratory of Reliability and Intelligence of Electrical Equipment, Hebei University of Technology, Tianjin 300401, China
* Correspondence: ydlian@hebut.edu.cn

Abstract: Tapered optical fibers have continuously evolved in areas such as distributed sensing and laser generation in recent years. Their high sensitivity, ease of integration, and real-time monitoring capabilities have positioned them as a focal point in optical fiber sensing. This paper systematically introduces the structures and characteristics of various tapered optical fiber sensors, providing a comprehensive overview of their applications in biosensing, environmental monitoring, and industrial surveillance. Furthermore, it offers insights into the developmental trends of tapered optical fiber sensing, providing valuable references for future related research and suggesting potential directions for the further advancement of optical fiber sensing.

Keywords: tapered optical fiber sensing technology; structure of tapered optical fibers; applications of tapered optical fibers

Citation: Ban, S.; Lian, Y. The Structure and Applications of Fused Tapered Fiber Optic Sensing: A Review. *Photonics* **2024**, *11*, 414. https://doi.org/10.3390/photonics11050414

Received: 13 March 2024
Revised: 17 April 2024
Accepted: 28 April 2024
Published: 30 April 2024

1. Introduction

As early as 1992, Birks et al. [1] proposed a model for stretching optical fibers into a tapered shape using different lengths of heat sources. Subsequently, tapered optical fibers have been explored in sensing. In recent years, optical fiber sensing technology has experienced vigorous development in various aspects such as multimodal integration [2], intelligence [3], adaptation [4], the introduction of new materials [5], nanotechnology [6], and quantum optics [7]. Among these, tapered optical fibers, due to their small size and unique tapered structure, tightly interact with external environments, demonstrating the capability for achieving ultra-high sensitivity measurements. Traditional sensors, while widely employed with mature manufacturing technologies, exhibit limited sensitivity, are constrained by active measurements, and are more susceptible to electromagnetic interference [8]. In contrast, tapered optical fiber sensors offer advantages such as being lightweight and small, exhibiting corrosion resistance and immunity to electromagnetic interference, as well as high measurement accuracy, low cost, and better compatibility, making them widely applicable in areas such as biosensing [9–11], environmental monitoring [12–14], and industrial surveillance [15,16].

The structure and performance of tapered optical fiber sensors are closely related, with subtle changes in structure having a significant impact on sensor performance. Multimode optical fibers with tapered structures have garnered attention in the sensing field for their high sensitivity and robust durability. By depositing a metal layer on the surface, the tapered structure can be adjusted to enhance measurement sensitivity [17], particularly exhibiting strong responses to variations in the vertical direction [18], making them suitable for various environmental monitoring applications [19,20]. Fiber Bragg Grating (FBG) utilizes the diffraction principle to modulate the refractive index (RI) of the optical fiber

periodically, forming a diffraction grating with high sensitivity and frequency selectivity, suitable for precise measurements of parameters for instance temperature and stress [21,22]. Long-period fiber gratings (LPBGs) achieve periodic structural changes by adjusting the RI, presenting a large response range and high sensitivity, which is especially suitable for displacement and pressure measurements [23,24]. Photonic Crystal Fiber (PCF), with its controllable microstructure arrangement, regulates the motion of photons, providing multifunctionality and stable performance in sensing applications, applicable to the detection of gases, liquids, and other media [25,26]. Optical tweezers capture microparticles by adjusting laser power, featuring advantages such as low cost and high efficiency, and are widely used in particle manipulation and levitation on a microscopic scale [27,28]. The Mach–Zehnder Interferometer (MZI) achieves high sensitivity sensing by measuring relative phase changes, suitable for measuring optical path differences [29,30]. The Fiber Loop Ringdown (FLRD) forms a light ring by connecting two optical couplers, achieving stable signal attenuation for rapid response and high sensitivity measurements [31,32]. The unique capabilities of these optical fiber structures play a crucial role in different application scenarios, providing vast possibilities for the continuous development of optical fiber sensing technology.

This paper provides a comprehensive review of tapered optical fiber sensing technology, starting from the principles and structures of sensors, and analyzing the advantages, potential challenges to be addressed, and parameters of different tapered optical fiber sensor structures. Additionally, it introduces some current applications of tapered optical fiber sensors and concludes by discussing the shortcomings of current tapered optical fiber sensors and potential directions for their development in practical applications.

2. Different Sensor Structures

Fabrication of tapered optical fibers involves stretching and melting single-mode or multimode fibers to form tapered structures, and the key lies in selecting appropriate techniques. Common methods include laser ablation (utilizing CO_2 [33], femtosecond technology [34], etc.), electron beam lithography [35], gas–liquid–solid technology [36], and fiber pulling [37], among others. Among these, flame heating technology is one of the most commonly used methods. By controlling the position, temperature, and stretching speed of the heating source, tapered optical fibers with different shapes can be obtained, suitable for various application fields, as shown in Figure 1. Therefore, the improvement of flame heating technology is particularly important. Felipe et al. [38] achieved a gradual reduction or stepped change in fiber diameter while ensuring uniform stretching through constant-speed flame brush scanning. Harun et al. [39] fabricated tapered optical fibers using flame brush technology, employing a butane–oxygen torch, microcontroller, and stepper motor. The improved system reduced the unevenness of tapered optical fibers, enabling simple and high-quality fabrication of tapered optical fibers.

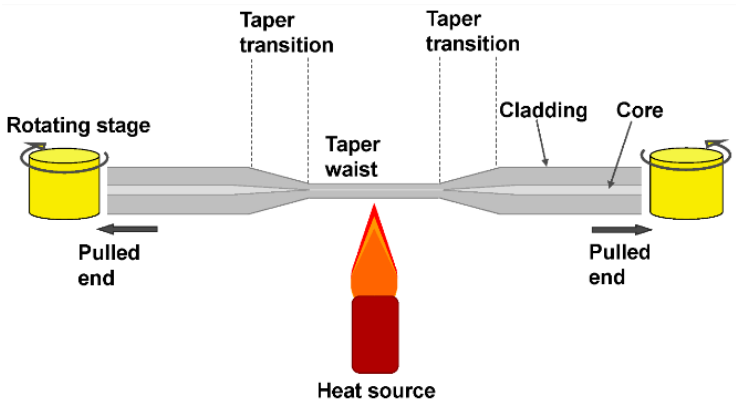

Figure 1. The schematic diagram for preparation of fused-tapered optical fiber [40].

Light propagates through the optical fiber in various modes, including core modes and cladding modes, which are coupled to one end of the tapered optical fiber. The other end is exposed to the test environment, such as liquids, gases, or biological samples. Physical or chemical parameters in the environment, for instance, temperature, pressure, RI, or chemical concentration, influence the propagation of light waves in the tapered optical fiber, leading to changes in its optical properties. Measurement of variations in reflected light intensity, phase changes, or spectral characteristics correlates with changes in environmental parameters, allowing the extraction of the desired information through analysis of the measurements.

The structure and performance of melted-tapered optical fiber sensors are closely related, and subtle changes in structure significantly impact the sensor's performance and functionality. In this section, melted-tapered optical fiber sensors are categorized based on MMFs, fiber gratings, PCFs, optical tweezers, and the principles of optical interference.

2.1. Multimode Fiber

Sensors employing a tapered structure with multimode optical fibers offer a broader application range and lower cost compared to single-mode fibers. Currently, a trending research direction involves the use of multimode optical fiber tapered sensors coated with different materials. In 2014, Shabaneh et al. [41] utilized a tapered multimode optical fiber coated with graphene oxide (GO) nanolayers to detect varying concentrations of ethanol-water solutions. The response exhibited strong reversibility and repeatability, with rapid response and recovery times as low as 19 s and 25 s, respectively, at room temperature. In 2015, Ibrahim et al. [42] employed a tapered multimode optical fiber coated with polyaniline nanofibers to differentially discern ammonia concentrations, achieving faster response times compared to known planar waveguide-based sensors. In 2016, Qiu et al. [43] utilized a tapered multimode optical fiber coated with a single-layer graphene film, realizing a cost-effective and portable molecular concentration detection sensor with reliable sensitivity, as illustrated in Figure 2. In 2023, Chauhan et al. [44] deposited a thin layer of SnO2-NP on a tapered multimode optical fiber for ethanol sensing, achieving an exceptionally high average sensitivity of 22 counts/ppm. This highlights the tremendous potential of coated tapered multimode optical fiber sensors in various applications.

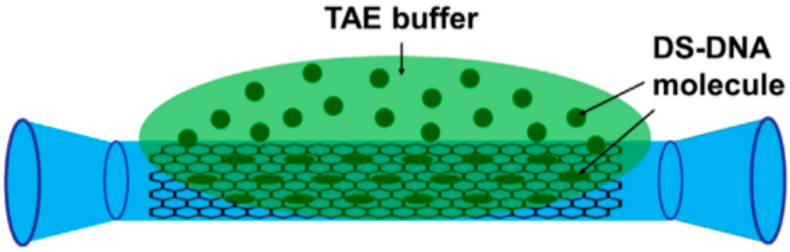

Figure 2. The tapered fiber core of TMMF was designed by Qiu et al. [43].

The Single-Mode to Multi-Mode to Single-Mode Fiber (SMF-MMF-SMF, SMS) structure, as an extension of multimode optical fiber, achieves efficient coupling between single-mode and MMFs by sandwiching an MMF between two single-mode fibers. The SMS structure incorporating a tapered configuration is similar to the conventional SMS structure, but it connects single-mode and multimode fibers through the tapered structure [45]. Figure 3 illustrates a basic diagram of the SMS structure.

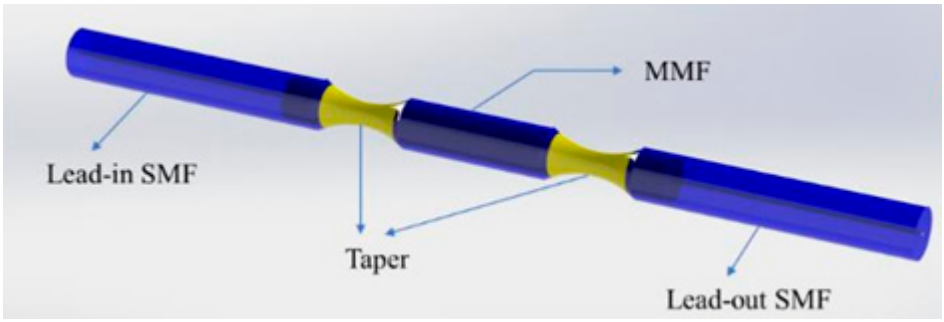

Figure 3. Schematic diagram of the structure of the tapered SMS [45].

The design of a tapered MMF eliminates the need for complex processes such as port reduction and offers higher durability against longitudinal strain when used in fiber refractometers. Simultaneously, the presence of MMF introduces mode coupling effects, enhancing the sensor's response to external environmental changes. In the tapered SMS structure designed by Sun et al. [18], the high resistance to a longitudinal strain of the refractometer reaches over 4000 με before failure. As the length of the MMF decreases, the sensitivity of the effective RI to the external RI increases, demonstrating significant potential applications. In the enhanced evanescent field fiber refractometer based on the SMS structure designed by Wang et al. [46], ultra-high sensitivity in the range of 1.33–1.44 for RI measurements was achieved (superior to 1900 nm/RIU when the RI is 1.44), making it the highest reported sensitivity in the literature at that time.

Researchers continue to explore the optimization of the tapered SMS structure. André et al. [47] proposed and experimentally demonstrated that gradually narrowing the SMS structure enhances sensitivity. They combined non-tapered and tapered SMS structures as a sensing system for simultaneous strain and temperature measurements. Zhao et al. [48] investigated a novel RI sensor based on a multi-tapered SMS fiber structure and found that the more tapers, the higher the measurement sensitivity. Yang et al. [49] sandwiched a balloon-shaped MMF formed by bending the tapered structure between two SMFs, as shown in Figure 4. By leveraging the advantages of tapering and bending, they designed a high-sensitivity refractive index sensor with a maximum sensitivity of 6909 nm/RIU (RI = 1.42). In addition to the SMS fiber, the combination of SMS with other optical structures also holds promising prospects. For instance, Song et al. [50] discovered that the process of writing FBG into SMS could be an effective technique for adjusting and optimizing the SMS spectrum for sensing purposes. We may anticipate witnessing examples of introducing tapering in FBG-in-SMS structures in the future to achieve enhanced sensitivity while optimizing the SMS spectrum.

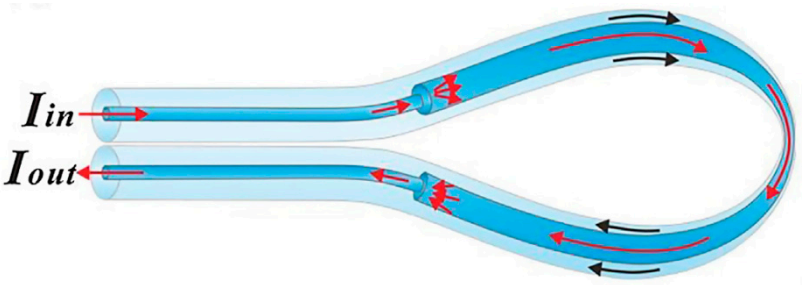

Figure 4. Schematic of the balloon STMS structure designed by Yang et al. [49].

The MMF structure plays a significant role in optical sensors. For instance, the extended design of the MMF structure, such as the SMS structure, enables the development of tapered optical fiber sensors with enhanced durability against longitudinal strain and improved sensitivity. These sensors have considerable potential in practical applications. However, this structure also requires consideration of factors such as mode overlap-induced

interference affecting sensor accuracy and stability [51], waveguide losses reducing signal transmission efficiency and sensor performance [52], and mode-coupling effects in MMF segments potentially leading to wavelength dependency of optical signals [53]. Therefore, the optimization of structures incorporating MMFs remains an ongoing area of research that requires continuous advancement.

2.2. Fiber Bragg Grating

In modern optics and sensing technology, FBG structures have become crucial tools. Among them, sensors based on FBG in tapered optical fibers and sensors utilizing LPBG structures, as two specific types of fiber sensors, have garnered widespread research interest and application exploration.

The structure combining tapered optical fibers with Fiber Bragg Gratings (FBGs) incorporates periodic refractive index modulation FBGs as the sensing element, which combines the large sensing area and high sensitivity of tapered optical fibers with the high resolution, selectivity, and sensitivity of FBGs. This has made it one of the highly researched directions in fiber optic sensing technology. Such a structure can optimize the response characteristics of FBGs, making them more suitable for specific application scenarios and providing more accurate measurements.

Yang et al. [54] achieved a pump efficiency higher than 0.21 °C/mW using gold nanoparticle-modified tapered optical fibers with FBGs while maintaining a local temperature rise of up to 60 °C under aqueous conditions, as shown in Figure 5. This provides a new approach for applications requiring local opto-thermal driving and real-time feedback of temperature fields. Zhao et al. [55] demonstrated a strain sensor based on a tapered FBG-capillary structure with a sensitivity of up to 1129.44 pm/με, which is approximately two orders of magnitude higher than that of conventional FP strain sensors. The FBG in the capillary, without strain, perfectly compensates for temperature effects. Li et al. [56] proposed an intensity-modulated, wide-bandwidth magnetic field fiber sensor based on Tapered Fiber Bragg Gratings (TFBGs), with a maximum sensitivity of −0.1933 dB/Oe and −0.1533 dB/Oe, as shown in Figure 6. It offers the advantages of no directional disturbance, wide bandwidth, high sensitivity, and integration.

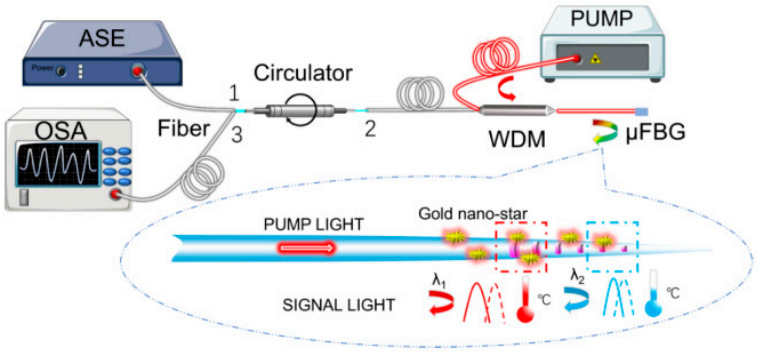

Figure 5. Schematic of the optical path of the sensor proposed by Yang et al. [54].

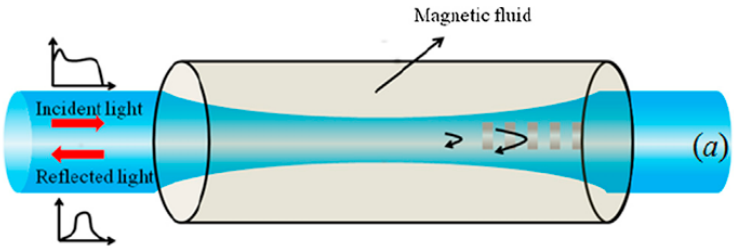

Figure 6. Structure of the TFBG magnetic field sensor proposed by Li et al. [56].

Tapered optical fiber sensors based on FBG have injected new momentum into the innovation and application expansion of fiber sensing technology. With technological advancements, FBG-based tapered optical fiber sensors are expected to achieve measurements for a broader range of parameters. Simultaneously, these sensors may acquire additional functionalities, such as structural health monitoring and environmental sensing, offering richer solutions for complex real-world applications.

Tapered optical fiber sensors based on LPBG utilize the diffraction effect of LPBG to couple light signals periodically with the physical or chemical parameters of the external environment, providing sensing capabilities [57]. In contrast to FBG sensors responding to changes at specific Bragg wavelength points, LPBG sensors typically exhibit variations over a larger wavelength range.

As early as 2007, Bock et al. [58] proposed a tapered LPBG pressure sensor. Compared to traditional FBG sensors, the manufacturing process of this tapered LPBG is simpler and faster. Additionally, this sensor allows for direct high-pressure measurements without the need to attach the grating to external strain components, thereby improving measurement accuracy. In 2010, Lee et al. [59] innovatively investigated coated LPBGs, applying a silicon film grating to a tapered optical fiber. The tuning efficiency of the sensor reached 62.9 nm/°C, equivalent to a sensitivity of approximately 168.182 nm/RIU, marking the highest sensitivity in fiber sensors at that time. The potential of tapered optical fibers combined with LPBG is evident. In 2023, Shao et al. [60] proposed a high-sensitivity dual-parameter tapered long-period fiber grating (MTLPG) sensor filled with magnetic fluid, as shown in Figure 7. The sensor exhibits different response ranges and sensitivities based on varying MF concentrations and MTLPG taper diameters, with maximum sensitivities reaching 23.72 nm/mT and 0.52 nm/°C, respectively. Additionally, the maximum response ranges extend from 8.0 to 16.0 mT and from 25 to 75 °C. To the best of our knowledge, this represents the highest magnetic sensitivity achieved by fiber optic sensors in weak magnetic fields (below 3 mT).

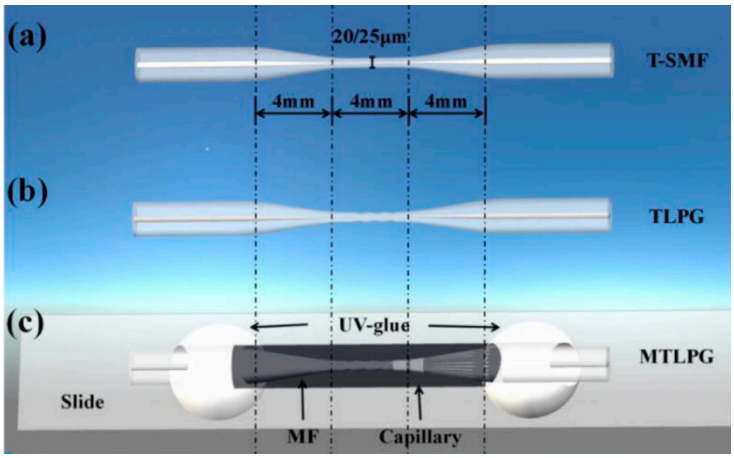

Figure 7. Fabrication diagram of the MTLPG dual parametric sensor proposed by Shao et al. [60].

Tapered optical fiber sensors based on Long Period Fiber Grating (LPBG) exhibit numerous advantages, such as the ability of LPBG resonance wavelength to vary with changes in the RI of the surrounding environment. This feature enables selective identification of different samples [61]. Moreover, these sensors typically do not require the addition of markers to the test samples, allowing for label-free detection. Consequently, LPBG-based tapered sensors will continue to contribute to the advancement of fiber sensing technology, providing solutions for tackling more complex real-world problems.

2.3. Photonic Crystal Fiber

The concept of PCF can be traced back to the 1990s [62]. As a deeper understanding of PCF microstructures and waveguide modes emerged, researchers began considering

its application in sensors. PCF tapered sensors involve the tapering of PCF with periodic RI structures [63], offering advantages such as high sensitivity, broad wavelength range, precise beam control, and versatility. Additionally, due to the non-conductive nature of PCFs, they exhibit increased stability in environments with electromagnetic interference and shielding [64].

The integration of the tapered section with the PCF occurs through different approaches. In the sensor design by Zhao et al. [65], the PCF between the upper tapered junctions undergoes etching, allowing the cladding modes of PCF to be excited through the upper tapered junction for RI sensing, as shown in Figure 8. Conversely, Fan et al. [66] directly employed PCF tapering for micro-strain sensing, effectively enhancing the sensor's sensitivity, as shown in Figure 9. It is noteworthy that prior to tapering, the strain sensitivity of the sensor was 2.75 με with a linear fit of 98.35%. After tapering, when the strain range was 5.46 pm/με, the strain sensitivity of the sensor improved to 98.59%, with a linear fit ranging from 109.860 με to 559.287 με. The improved strain sensor exhibits high sensitivity, good stability, quick response speed, and excellent reversibility, thus holding significant potential for broad applications.

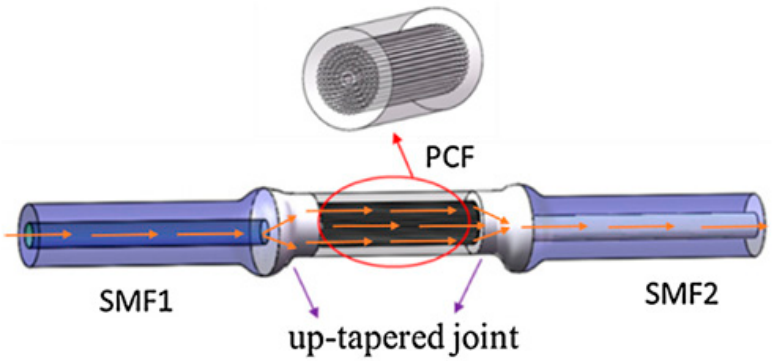

Figure 8. Schematic diagram of the upper tapered junction sensor designed by Zhao et al. [65].

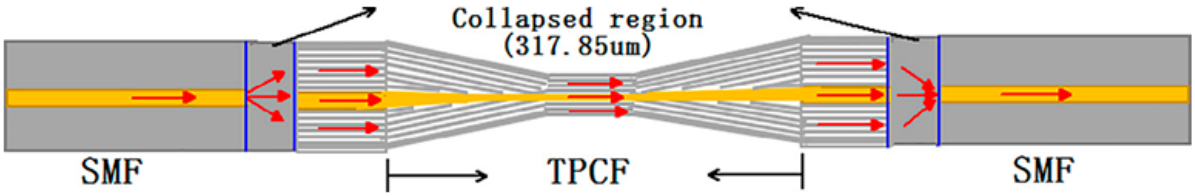

Figure 9. Schematic diagram of the sensor designed by Fan et al. [66].

Combining PCF microcavities with tapered optical fibers allows for the exploitation of the microcavity's high-quality factor and optical characteristics, leading to sensors with enhanced sensitivity. Dass et al. [67] devised a curvature sensor based on a cascaded single-mode fiber with microcavities and dual-tapered spliced PCF. The dual SMF tapers elevated the system's curvature sensitivity while customizing the curvature sensitivity and interference fringe contrast could be achieved by altering the taper parameters of the second taper. With technological advancements, researchers have explored PCF sensors capable of simultaneously sensing multiple parameters, enhancing measurement efficiency, and broadening application possibilities. Fan et al. [25] proposed a dual-parameter sensor for liquid level and RI using an SMF-TPCF-SMF structure. Leveraging PCF's temperature-insensitive characteristics, the sensor addressed crosstalk caused by temperature variations. As a dual-parameter sensor, its structure is relatively simple, yet it exhibits excellent sensing performance.

In addition to the two common designs mentioned above, Tu et al. [68] proposed a non-traditional type of PCF tapered RI sensor by using atomic layer deposition to coat a one-dimensional photonic crystal consisting of periodic TiO_2 and Al_2O_3 on a tapered optical

fiber. This represents the first demonstration of a fiber-based Bloch surface wave-excited sensor for RI sensing.

Currently, there are also popular research directions in sensing based on PCF combined structures, such as magnetic sensing based on PCF tapered Mach–Zehnder interferometer structure [69], and surface-enhanced Raman spectroscopy sensing based on PCF [70]. With the continuous advancement of technology, PCF tapered sensors are expected to discover opportunities in new fields such as quantum technology and photonic integration. However, when applying PCF tapered sensors in real-world environments, consideration must be given to factors such as stray light, humidity, and gases, which can impact the performance of the sensor.

2.4. Optical Tweezers

The optical fiber tweezer is an optical trapping and sensing device that utilizes light manipulation for capturing particles or micro-objects. Optical tweezers designed with a tapered fiber structure can enhance trapping forces and control the position and movement of captured particles [71], providing a powerful tool and means for research and applications at the microscale. Figure 10 illustrates several basic schematics of optical tweezers.

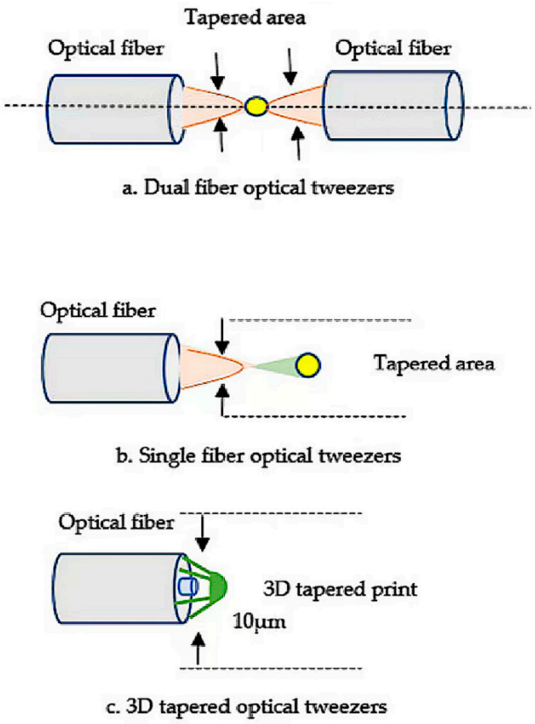

Figure 10. Tapered optical fiber based on optical tweezers structure [72].

By altering the arrangement and combination of fibers within the optical tweezer, the functionality of the optical tweezer can be modified. Huang et al. [73] achieved optical trapping and manipulation of Escherichia coli cells using a tapered fiber with a dual-fiber arrangement, forming a high-energy density crossing point and utilizing gradient forces. Directional control of bacterial cells was achieved by adjusting the power in the fiber probe to direct cells in different directions. Gao et al. [27] achieved both single-fiber gradient mode and dual-fiber scattering mode trapping configurations in a single optical tweezer setup based on a tapered optical fiber, as shown in Figure 11. This configuration enables the trapping and manipulation of at least three particles simultaneously, each of which can be utilized for in-situ experimental activities and analyses, holding significant implications for super-resolution imaging based on microsphere-assisted techniques.

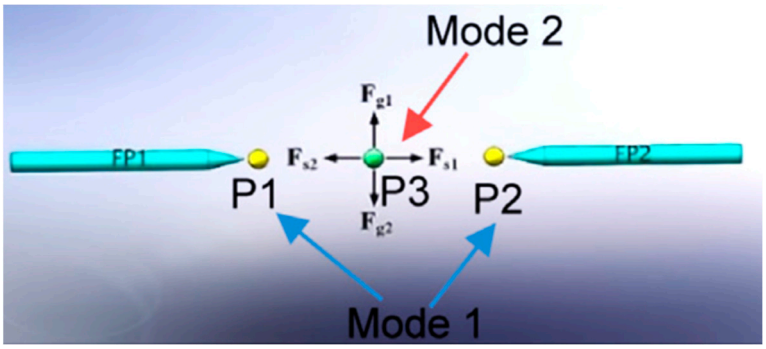

Figure 11. Schematic diagram of the dual-trapping mode of an optical tweezer [27].

Additionally, changing the type of fiber can diversify the functionalities of the optical tweezer. Liu et al. [74], by introducing radial offset between a single-mode fiber and a graded-index MMF with a tapered tip, achieved both non-contact operation and the capability to axially displace particles relative to the fiber tip without moving the probe. Similarly, based on RI and MMFs, Wang et al. [75] utilized a graded RI MMF tweezer for three-dimensional trapping of yeast cells, adjusting the position of trapped particles by modifying the fiber tip. Rong et al. [76] developed an optical tweezer based on a large-diameter four-mode fiber, allowing the extension of resonant fields of higher-order modes for manipulating micro-objects. It is noteworthy that Rong et al. also demonstrated that a larger tapered fiber diameter can prolong the lifetime of the tweezer.

In addition to the fundamental optical tweezers, Asadollahbaik et al. [77] achieved efficient optical trapping and manipulation of micro-particles in a dual-fiber optical tweezer by incorporating a specially shaped diffractive Fresnel lens. The diffractive structure not only increased the trapping stiffness of the dual-fiber optical tweezer but also expanded the operational space for optical trapping. By integrating plasmonics, Fooladi et al. [78], leveraging the intrinsic field enhancement effects, demonstrated that the proposed tapered dual-core fiber tweezer can exert forces on particles with a radius as small as 0.01 μm, as shown in Figure 12.

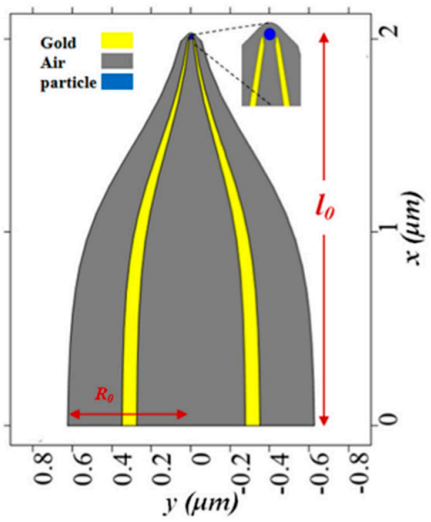

Figure 12. Cross-section of the tapered dual-core fiber proposed by Fooladi et al. [78].

As a crucial experimental technique, optical tweezers have not only propelled advancements in fundamental science but also provided innovative research and application opportunities across multiple domains. Despite significant progress in optical tweezer technology, challenges persist, such as potential sample damage due to beam energy and thermal effects [79], limitations of in-depth resolution and precise control in three-dimensional

manipulation, and the yet unrealized goals of automation and high-throughput operations. Future research and technological innovations will focus on addressing these limitations to further expand the applications of optical tweezers in micro-manipulation and biological research fields.

2.5. Fiber Interferometer

Both the FLRD and MZI are optical sensors based on the interference principles of light, exhibiting vast prospects for development in sensing performance, application domains, and material technologies.

The FLRD is a fiber optic sensing technique employed for detecting the absorption and scattering characteristics within a medium. In FLRD technology, optical pulses are injected into a fiber loop, and the attenuation time of the pulses is monitored to measure the absorption or scattering of light within the medium [80]. Early FLRD techniques were primarily based on traditional fiber loops, used to measure the decay time of light within the fiber loop to obtain information about the medium's absorption and scattering [81]. Subsequently, researchers introduced tapered optical fibers into FLRD technology, where the tapered end of the fiber can increase the interaction path between light and the medium, thereby enhancing sensitivity to the absorption and scattering of the medium [82].

In recent years, researchers have further improved the sensitivity and detection capabilities of FLRD technology by optimizing the structure, fabrication processes, and optical parameters of tapered optical fibers. For instance, Li et al. [83] utilized a bent tapered optical fiber to enhance the decay effect of the signal, achieving high-precision RI measurement through the cascading of an S-shaped optical fiber taper and a Faraday rotation mirror. Yang et al. [31] utilized a bent-annealed taper no-core fiber (NCF) immersed in magnetic fluid (MF) as the sensing head to construct a novel FLRD-based current sensing system, as shown in Figure 13. This configuration significantly enhances the evanescent field effect, resulting in a measurement sensitivity of 0.1161 μs/mA for the current sensor. Their contribution to the research and application in the field of modern electrical engineering is substantial.

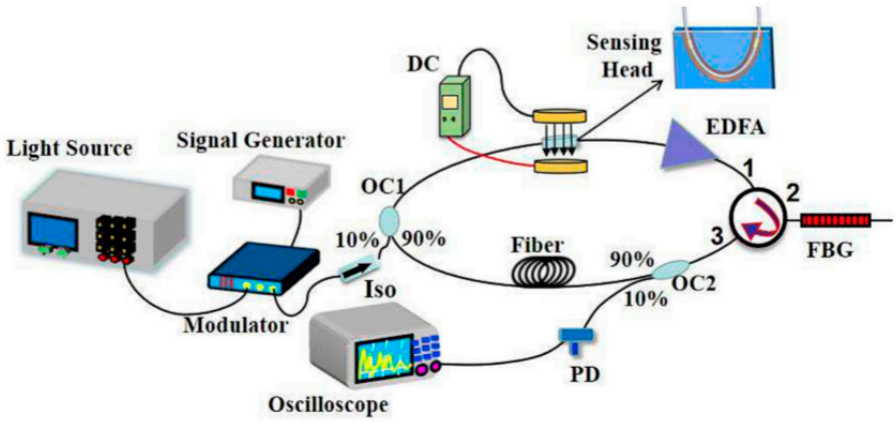

Figure 13. Schematic diagram of fiber-optic current sensor proposed by Yang et al. [31].

Simple tapered single-mode fibers, when combined with other optical fibers or structures, can also enhance FLRD systems. Tian et al. [84], for example, designed a chaos-correlated FLRD RI sensing system based on a tapered single-mode fiber. The chaotic correlation design simplified the light source of the sensing system, eliminating the trade-off between the length of the fiber loop and the light source and making the fiber loop length more flexible. Meanwhile, Wang et al. [85] used a tapered single-mode fiber and a thin silica MMF coated with polydimethylsiloxane as curvature and temperature sensors, achieving simultaneous measurement of both variables in a quasi-distributed sensing scheme.

The combination of FLRD technology with Frequency Shift Interferometry (FSI) is also a trending research direction, providing enhanced methods for the sensitivity, multi-

channel monitoring, and real-time data acquisition of sensors. Cheng et al. [86] integrated FLRD sensors with frequency-shifted interferometric measurements for large-strain measurements, achieving a sensitivity of 0.34 $km^{-1} \cdot m\varepsilon^{-1}$ and a dynamic range of 5 me. Chen et al. [87] similarly combined FLRD sensors with FSI for large-strain measurements, utilizing a dual-tapered multimode optical fiber as the sensor head. They achieved strain sensitivities of 0.51337 $km^{-1} \cdot m\varepsilon^{-1}$ and 0.8667 $km^{-1} \cdot m\varepsilon^{-1}$ within a large measurement range of up to 6 me, surpassing the design range and sensitivity of Cheng et al., while also enabling multi-point measurements.

In summary, FLRD systems combined with tapered optical fibers offer several unique advantages, such as rapid response, flexible design, and real-time monitoring capabilities. In the future, FLRD systems are expected to undergo further optimization in aspects like multi-channel and array integration [88], real-time monitoring, and data analysis, showcasing additional benefits and potential.

The MZI is an optical interference device typically composed of two beam splitters and two interference arms [89]. In traditional MZIs, conventional optical fibers or waveguide devices are used to construct the interference arms. When tapered optical fibers are introduced, they can act as special sensing elements within the interference arms, achieving highly sensitive sensing by intensifying the interaction between the optical field and the external environment. For instance, Wang et al. [90] enhanced the performance of the MZI in RI measurements by tapering the fusion point of the MZI, achieving good linearity, repeatability, and sensitivity, as shown in Figure 14.

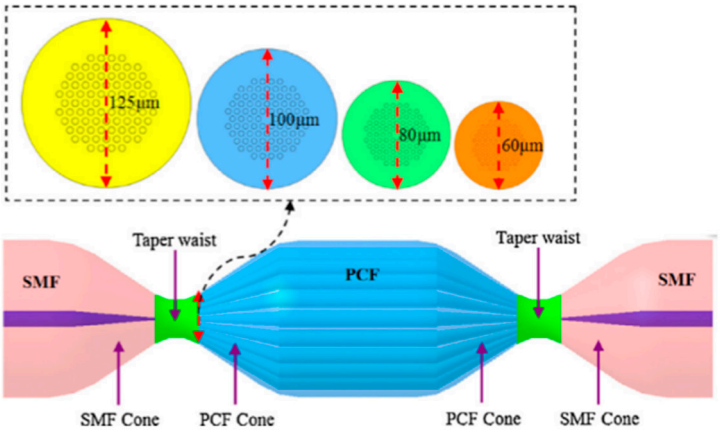

Figure 14. Schematic diagram of the spliced-point tapered single-mode fiber (SMF) to photonic crystal fiber (PCF) to single-mode fiber (SMF) MZI [90].

In optical fiber sensing, especially in RI measurements, temperature drift significantly impacts the accuracy and stability of the results. Mitigating the temperature drift in the MZI is an effective approach to enhance the stability, accuracy, and reliability of fiber optic sensors. Pawar et al. [91] reduced the temperature sensitivity of the MZI using tapered birefringent PCFs, simultaneously improving resolution and RI measurement, as shown in Figure 15. Yang et al. [92] achieved an MZI with lower temperature sensitivity by embedding a refined optical fiber, exhibiting sensitivity ten times higher than conventional tapered LPBG sensors. Additionally, Yang et al. observed that decreasing the diameter of the refined optical fiber and increasing the interferometer length further enhanced sensitivity. Wang et al.'s [93] research, based on folded tapered multi-mode coreless optical fiber, overcame temperature sensitivity while utilizing the compound interference of the MZI, significantly improving sensing performance in the low RI range. Within a linear RI range of 1.3405 to 1.3497, a maximum sensitivity of 1191.5 nm/RIU was achieved, surpassing traditional modal interferometer structures.

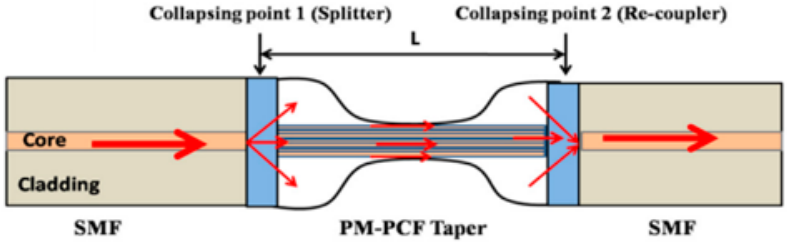

Figure 15. Schematic diagram of tapered PM-PCF fiber by Pawar et al. [91].

The application of tapered optical fibers in the MZI has introduced new possibilities in optical sensing. Its advantages lie in high sensitivity, high resolution, compact structure, and strong adaptability. However, the challenge remains in expanding the dynamic range while maintaining high sensitivity.

2.6. Summary

The parameters commonly used for tapered optical fiber sensors include the taper length, sensitivity, RI or wavelength scale, waist diameter, etc. Different types of sensors emphasize different parameters, and the specific selection depends on the requirements of the application. Table 1 provides a classification study of tapered optical fiber structures.

Table 1. Classification study of tapered fiber structures.

Tapered Method	Taper Length	Sensitivity	RI Scale OR Wavelength Scale	Waist Diameter	Application	Ref
MMF	2500 µm	3264.01 nm/RIU	1.345–1.375	40 µm	Biological and chemical	[17]
MMF	——	12145 nm/RIU	1.3345–1.339	4.2 µm	Biological and chemical	[94]
MMF	160 µm	11792 nm/RIU	1.3330–1.4102	——	Biological and chemical	[95]
FBG	7.29 mm	382.83 dB/RIU and 9.893 pm/°C	1.34974–1.35845	39 µm	Biological and chemical	[96]
LPBG	2.3 mm	Peak A 1.82 pm/µε, 47.9 pm/°C, Peak B 8.17 pm/µε, 65 pm/°C	Peak A: 1540.3–1543.2 nm, Peak B: 1571.4–1575.3 nm	62.5 µm	Temperature and strain	[97]
LPBG	1 mm	1246.594 nm/(N/mm)	1480–1640 nm	100 µm, 90 µm, 80 µm	Lateral Load	[23]
LPBG	690 µm	4.5 nm/(µg/mL)	1300–1620 nm	45.51 µm	Biomedical	[98]
PCF	10 mm	722.3 nm/RIU	1.30864–1.32014	18.1 µm	Biological	[99]
PCF	——	152.97 nm/RIU	1.330–1.383	40 µm	RI	[100]
FLRD	785 µm	2646.307 dB/(km RIU)	1.3330–1.3518	70 µm	RI	[83]
FLRD	340 µm	0.725 µs/m^{-1}	——	44.1 µm	Curvature	[101]
MZI	690–850 µm	−15.66 nm/µC	——	28–40 µm	Temperature	[102]
MZI	——	103.2 pm/°C	1.34–1.38	84.70 µm	Temperature	[103]
MZI	500 µm	0.116 nm/°C	——	80 µm	Temperature	[104]
MZI	——	4234 nm/RIU	1.4204–1.4408	35.5 µm	Biological and chemical	[105]

In summary, these fiber optic sensors exhibit high sensitivity and versatility in various application domains. However, they also come with limitations such as specific application requirements, complex manufacturing processes, and sensitivity to environmental conditions. For instance, PCF tapered sensors are limited by certain length constraints, optical tweezers require complex optical systems and are subject to sample character-

istics, and MZIs have a complex optical layout, being sensitive to light source stability and interference.

In addition to the mentioned tapered fiber optic sensor structures, there are other common tapered fiber optic sensors, such as surface plasmon resonance tapered fiber optic sensors [106], fiber optic surface-enhanced Raman scattering sensors [107], fiber optic Fresnel diffraction sensors [108], and fiber optic microsphere resonant sensors [11]. These tapered fiber optic sensors are currently in continuous development and research stages. Future advancements aim to enhance performance, reduce costs, expand application ranges, and address current limitations. They are poised to play a crucial role in various fields such as biomedical applications, environmental monitoring, industrial applications, and scientific research.

3. Applications

As an innovative optical sensing technology, tapered fiber optic sensors demonstrate extensive potential across various domains. For instance, the geometric structure of tapered fiber optics renders them highly sensitive to environmental changes, enabling real-time and high-sensitivity monitoring of parameters such as temperature and humidity. Additionally, by introducing specific materials or coatings to the surface of tapered fibers, accurate monitoring and analysis of substance concentrations and gas compositions can be achieved, providing a reliable means for biosensing and industrial production monitoring. This chapter introduces the applications of tapered fiber optic sensors in areas such as biosensing, environmental monitoring, and industrial surveillance.

3.1. Biosensing

In recent years, advancements in micro-nanofabrication technologies have propelled the rapid development of tapered fiber optic sensing techniques. The small size and high sensitivity of tapered fiber optics make them excellent candidates as sensitive detectors for the interaction of biological molecules. Through surface modifications, tapered fiber optics can achieve highly selective recognition of biomolecules, providing novel and crucial tools for biological research and clinical diagnostics. This section will showcase the potential applications of tapered fiber optic sensors in three aspects: detection of biomolecular concentrations, targeted drug delivery to cells, and DNA hybridization.

3.1.1. Biomolecule Concentration Detection

With the increasing demand for molecular detection within medical research, researchers have begun exploring the use of tapered optical fibers for the detection of biological molecules such as the specific binding of antigens and antibodies, as well as the activity of bacteria. Utilizing tapered optical fiber sensors, the detection of biological molecules has streamlined experimental cycles, making it more suitable for high-throughput analytical requirements.

By modifying the surface of tapered optical fibers with antibodies, antigens, and other biomolecules, real-time monitoring of their interactions can be achieved. This has significant applications in immunological research, drug screening, and diagnostic testing. As early as 1992, Ogert et al. [109] developed tapered optical fiber biosensors using specific antibodies and fluorescent signals, enabling rapid and sensitive detection of botulinum toxin. In 2019, Minkovich et al. [99] designed a non-adiabatic tapered special PCF, employing the interaction between a thin layer coated with bovine serum albumin (BSA) antigen and anti-BSA antibodies. This groundbreaking approach achieved a detection limit of 125 pg/mL for anti-BSA antibody concentration at that time. In the same year, Duan et al. [110] proposed a compact S-cone optical fiber biosensor, which marks the first integration of Hydrophobin I (HGFI), a hydrophobic protein found in Trichoderma reesei, onto an optical fiber, enabling label-free detection of the interaction between goat anti-rabbit immunoglobulin G (IgG) (GAR, antibody) and rabbit anti-coagulant IgG (R, antigen). The nanolayer of HGFI on the fiber surface provides a unique analytical platform for achieving biocompatible binding.

In 2023, Chen et al. [111] introduced a cone-shaped optical fiber biosensor based on the Mach–Zehnder Interferometer (MZI), incorporating a U-shaped transmission structure to realize a miniaturized plug-in probe that is flexible, convenient, and consumes minimal liquid, as shown in Figure 16. The cone probe achieved a sensitivity of 1611.27 nm/RIU within the refractive index detection range of 1.3326–1.3414, with an immunoanalytical detection limit of 45 ng/mL for different concentrations of human immunoglobulin G.

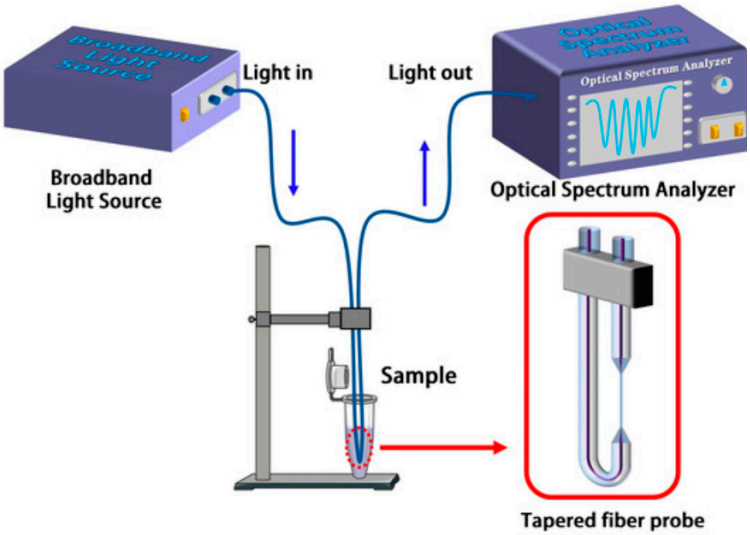

Figure 16. Schematic diagram of the conical fiber optic bioprobe experimental setup [111].

In the realm of microbiological research, tapered optical fiber sensors find applications in monitoring the dynamic activities of microorganisms such as bacteria and fungi. This proves instrumental in gaining insights into the ecological characteristics and antibiotic sensitivity of these microorganisms. In 2020, Chen et al. [112] introduced an exceptionally sensitive sensor utilizing a coreless tapered optical fiber functionalized with guinea pig immunoglobulin G antibodies for the detection of inactivated Staphylococcus aureus, as shown in Figure 17. The sensor exhibited a detection limit of 3.1 CFU/mL, marking the highest detection limit among optical fiber biosensors at that time.

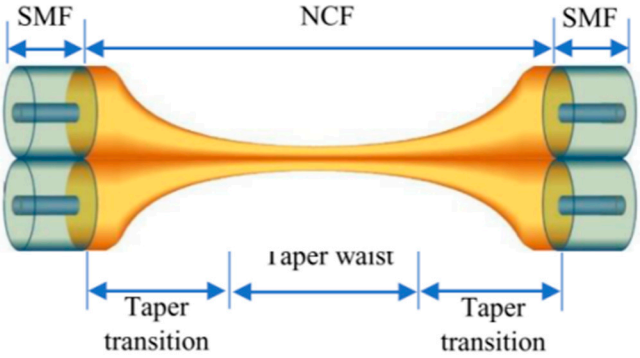

Figure 17. Schematic of the fiber structure designed by Chen et al. [112].

In 2021, Cui et al. [113] developed a quantum dot immunofluorescent tapered biosensor probe for the detection of Staphylococcus aureus, achieving a detection limit of 1×10^4 CFU/mL, as shown in Figure 18. Moving forward to 2022, Li et al. [114] designed a dual-cone microfiber MZI for Staphylococcus aureus detection, with a remarkable RI sensitivity of 2731.1 nm/RIU. The microfiber MZI, functionalized with porcine immunoglobulin, demonstrated specific binding to Staphylococcus aureus, achieving a low detection limit of 11 CFU/mL.

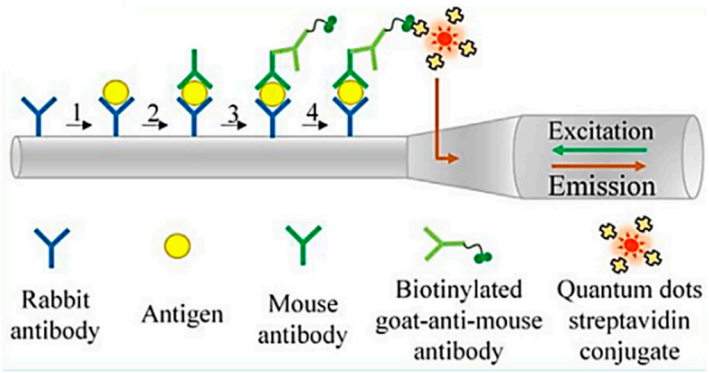

Figure 18. Principle of fiber probe for identification of Staphylococcus aureus [113].

The tapered optical fiber sensor exhibits numerous advantages in the realm of biomolecular concentration detection. Its simplicity in experimental operations renders it applicable to various settings, both within and outside the laboratory, making it suitable for diverse applications [115]. Additionally, it requires relatively small sample volumes, making it well suited for the analysis of precious or rare biological samples. In the future, researchers are actively exploring the integration of tapered optical fiber sensors into compact systems, aiming to enable real-time monitoring of biomolecular concentrations in on-site or clinical environments.

3.1.2. Cellular Realization of Targeted Drug Delivery (Cancer)

Research on tapered optical fiber sensors for DNA in situ detection in early cancer diagnosis is extensive. However, the field of targeted drug delivery using tapered optical fiber sensors remains an area requiring further exploration. This application aims to combine tapered optical fiber sensors with drug carriers to enable monitoring and control of drug release, thereby enhancing the precision and efficiency of treatment—a prospect that should not be overlooked.

In 2019, Liu et al. [116] efficiently and accurately achieved targeted drug delivery to individual cancer cells in vitro using tapered optical fiber probes, as shown in Figure 19. Simultaneously, they recorded the activity characteristics of targeted cancer cells upon drug exposure. Overcoming the challenges of low efficiency in targeted drug delivery and poor Raman spectral stability caused by Brownian motion, they utilized another fiber tip for optical manipulation of individual suspended cells.

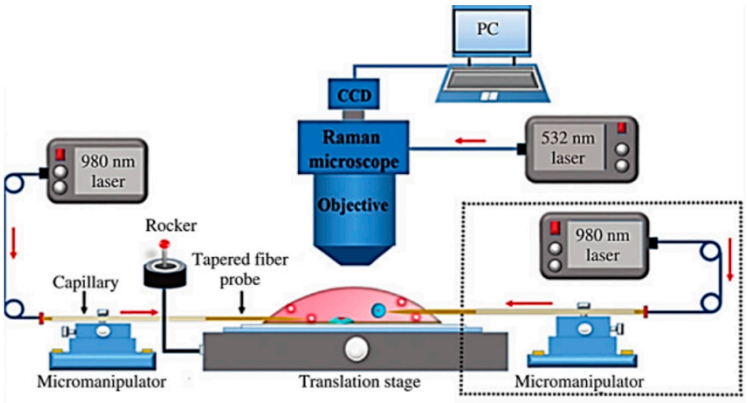

Figure 19. Schematic of the experimental setup set up by Liu et al. [116].

In pursuit of a more comprehensive approach to cancer treatment, in 2023, Vikas et al. [117] designed a graphene-antimony-coated uniform waist-tapered optical fiber surface plasmon resonance biosensor. In contrast to Liu et al.'s design, which focused on manipulating individual cancer cells, Vikas et al.'s design can detect various cancer cells

within the human RI range of 1.36–1.4. The high binding energy and large active surface area of antimony for adsorbing biomolecules enhance the sensor's performance. However, this design still requires further exploration in terms of drug delivery functionality.

3.1.3. DNA Hybridization

DNA hybridization is a crucial step in the detection and analysis of specific DNA sequences. Tapered optical fiber sensors, leveraging the high sensitivity of the fiber cone structure and surface functionalization capabilities, enable monitoring and analysis of the DNA hybridization process. There is a continuous effort to enhance the sensitivity and detection limits of these sensors.

The detection of DNA hybridization can be achieved through various tapered optical fiber structures. Pan et al. [118] utilized a portable and rapidly manufactured single-mode tapered optical fiber to monitor changes in the surrounding RI, facilitating basic DNA molecule measurements. On the other hand, Sun et al. [119] employed a reflection microfiber Bragg grating (mFBG) structure to achieve highly specific DNA hybridization detection. By monitoring the wavelength gap between two well-defined resonances in the reflection provided by the mFBG, they implemented temperature-compensated RI measurements, thereby enhancing the accuracy and reliability of the detection results.

To further optimize the sensitivity and detection limits of the sensor, Li et al. [29] demonstrated that reducing the core size through tapered shaping significantly enhances the RI sensitivity of the sensor. Additionally, through integration with other optical structures such as MZIs, real-time, highly sensitive, and ultra-low detection limit detection of DNA can be achieved. Song et al. [120] proposed an unlabeled DNA biosensor based on microfiber MZI, whose interference spectrum is highly sensitive to RI changes. With a detection limit as low as 0.0001 pmol/μL at an RI of around 1.34.

Modifying the fiber optic structure or surface functionalization can enhance the specificity of the sensor. In 2018, Zainuddin et al. [121] functionalized the tapered region of a fiber optic sensor using sodium hydroxide, triethoxysilane, and glutaraldehyde, achieving highly specific detection of Helicobacter pylori DNA, as shown in Figure 20. In 2019, Zhang et al. [122] employed a single-layer poly-L-lysine and single-stranded DNA probe for functionalizing double-S tapered optical fibers based on microcore fibers, demonstrating excellent specificity and reproducibility in label-free DNA hybridization detection. In 2023, Zainuddin et al. [123] further developed a carbon quantum dot-enhanced sensor for the detection of Helicobacter pylori DNA, as shown in Figure 21. With a detection limit of 1.0 fM, the sensor exhibited a favorable sensitivity of 1.8295 nm/nM and a low dissociation constant. Moreover, it demonstrated higher affinity compared to biosensors without the use of carbon quantum dots (CQDs). This sensor not only showcased the significant role of nanomaterials in sensor enhancement but also emphasized the potential for more sensitive and reliable diagnostics in Helicobacter pylori infections. It provides a new direction for the development of medical sensors, highlighting the potential for enhanced sensitivity and reliability in Helicobacter pylori diagnosis tests.

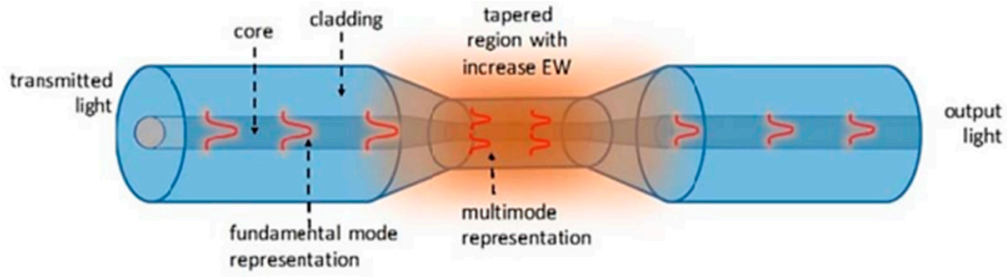

Figure 20. Schematic of light propagation in a tapered fiber [121].

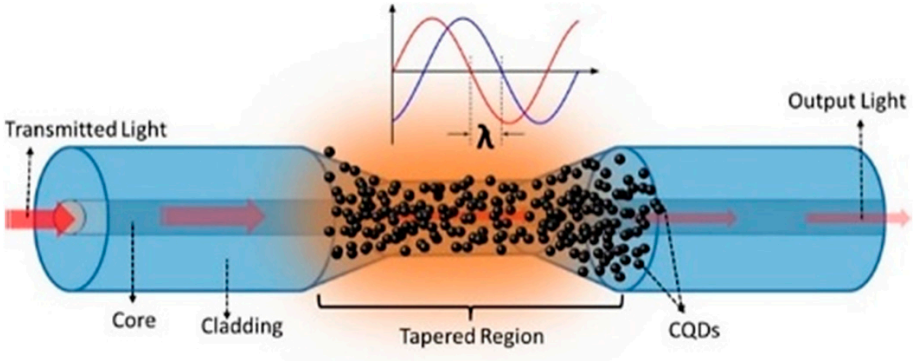

Figure 21. Schematic of light propagation in a CQD-functionalized tapered fiber [123].

3.2. Environmental Monitoring

Tapered optical fiber sensors enable high-precision measurements of environmental parameters, capturing subtle changes in the surroundings and providing accurate data support for both scientific research and practical applications. Through the adjustment of sensitive coatings on tapered optical fibers and optimization of fiber design, real-time, high-precision monitoring of environmental parameters such as temperature, humidity, and water pollutants can be achieved.

3.2.1. Ambient Temperature and Humidity Sensing

The measurement of environmental temperature and humidity is not only crucial for scientific research but also finds applications in urban planning, environmental management, and natural resource conservation, contributing to the improvement of environmental quality and the enhancement of overall quality of life. Tapered optical fiber sensors can perceive changes in environmental humidity by monitoring variations in hygroscopic materials and can detect changes in environmental temperature utilizing the thermal-sensitive characteristics of optical fibers.

As early as 1998, Bariain et al. [124] developed a novel humidity optical fiber sensor by depositing a hygroscopic material (CoCl2) onto a small region of a tapered optical fiber, observing a significant output optical power change of up to 5 dB. Subsequently, researchers have enhanced sensor sensitivity by combining tapered optical fibers with specific sensitive materials to obtain more precise environmental data. Li et al. [125] proposed an interferometric sensor using an SMF-PCF-SMF structure, achieving humidity measurement through the fusion of tapered coupling and graphene coating. Within a humidity range of 36.0% RH to 75.3% RH, the sensor exhibited high sensitivity, reaching 340.13 pm/% RH. Quiñones-Flores et al. [126] designed a relative humidity (RH) sensor based on the multimode interference (MMI) phenomenon using a coreless optical fiber (NCF) coated with polyvinyl alcohol (PVA), as shown in Figure 22. The sensor consisted of a segment of NCF spliced between two single-mode fibers (SMFs). The native MMI sensor exhibited a sensitivity of 5.6 nm/RH% in the range of 87% to 93% RH, while the tapered MMI sensor demonstrated a higher sensitivity of 6.6 nm/RH% in the range of 91.5% to 94% RH. To the best of our knowledge, the sensitivity values obtained using these MMI sensors in similar RH ranges are at least twice that of the most sensitive fiber humidity sensor reported in the literature.

By employing special structural designs, the performance and practical applicability of sensors can be effectively enhanced. Le et al. [127] combined MMF and SMF cones and, through specific knotting and PVA coating processes, designed a multimode microfiber nodal resonator sensing probe. In a microfiber with a diameter of 4 μm, the effective RI difference between the HE11 and HE12 modes was nearly zero. Kou et al. [128], based on a reflective Fabry–Perot mode interferometer, designed an ultra-compact all-silicon high-temperature sensor. The sensor head, compact and splice-free, can operate in harsh environments with extremely large temperature gradients. However, further research

and improvement are still required for the practical implementation of this excellent design, such as enhancing its stability and protective performance through encapsulation techniques. Tong et al. [129] combined FBG with an internally embedded balloon-like sensing structure for simultaneous measurement of relative humidity and temperature, as shown in Figure 23. Compared to traditional sensing structures, the balloon-like sensing structure not only offers better contact with the measurement environment but is also simple to manufacture and cost-effective.

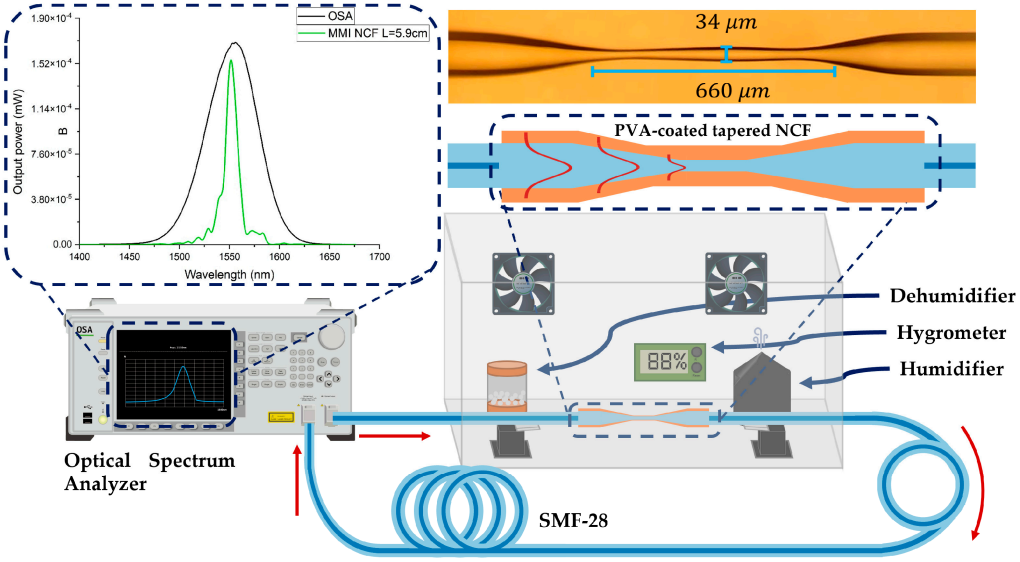

Figure 22. Experimental set-up by Quiñones-Flores et al. [126].

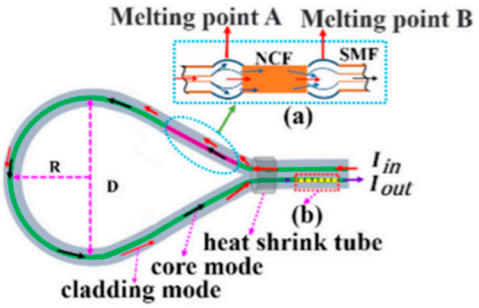

Figure 23. Schematic diagram of a two-parameter simultaneous measurement sensing structure with (**a**) embedded MZI and (**b**) FBG [129].

3.2.2. Detection of Ethanol Concentration in Water

Excessive ethanol concentration in water bodies, stemming from wastewater discharge, industrial production, and agricultural activities, can lead to pollution and harm the water quality, impacting aquatic ecosystems and biodiversity. The real-time and high-sensitivity monitoring of ethanol concentration in water can be achieved using tapered optical fiber sensors, contributing to the protection of water environments.

Traditional methods rely on the absorption characteristics of optical fibers to detect ethanol concentration. Building upon these traditional methods, Yang et al. [130], through V-number matching and optimization of cone radius and length, enhanced the sensitivity of ethanol concentration sensors. With technological advancements, researchers have begun exploring the application of surface plasmon resonance (SPR) technology in fiber optic ethanol sensing. For instance, Semwal et al. [131] designed a tapered optical fiber ethanol sensor based on localized surface plasmon resonance, combined with gold nanoparticle coating and enzyme immobilization. This sensor is capable of detecting ethanol in water and measuring ethanol concentration in human bodily fluids.

Presently, researchers are incorporating nanomaterials into optical fiber sensors to enhance sensitivity and selectivity. Azad et al. [132], by coating tapered optical fibers with ZnO nanorods, shortened the sensor response time to 0.6 s and increased linearity to 97%, as shown in Figure 24. Similarly, Khalaf et al. [133] coated tapered optical fibers with carbon nanotubes and GO films, simplifying sensor implementation and ensuring sensitivity. Simultaneously, the sensors exhibited excellent selectivity for ethanol across various organic compounds.

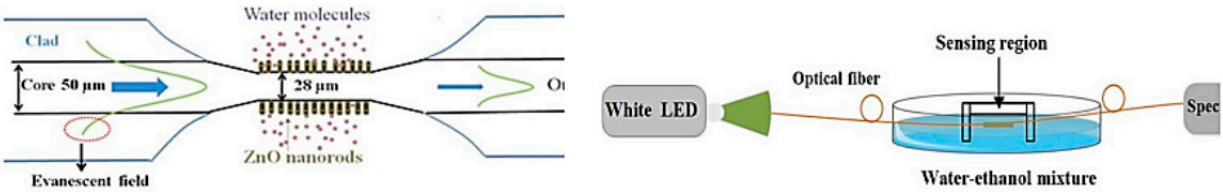

Figure 24. (**a**) Schematic of the sensing area of the sensor of Azad et al.; (**b**) setup of the experimental apparatus [132].

Consideration needs to be given to the fact that, in the detection of ethanol concentration, sensors may be influenced by other environmental factors such as temperature, humidity, and the presence of other gases. Future research endeavors should continue to advance in overcoming cross-interference to enhance the robustness and accuracy of ethanol concentration measurements.

3.3. Industrial Monitoring

Tapered optical fiber sensors exhibit high sensitivity, rapid response, high-temperature resistance, corrosion resistance, real-time monitoring, and remote operation advantages in industrial production monitoring and control. These attributes contribute to the optimization of production processes and enhance production efficiency and quality control.

3.3.1. Radiation Dosimetry

Tapered optical fibers, as a highly sensitive sensing platform, exhibit extensive potential in radiation dose measurements, offering high precision, spatial resolution, and real-time monitoring capabilities. Researchers continuously explore innovative methods for detecting charged particles of different energies and types. In 2021, Jia et al. [134] successfully measured remote γ-ray doses by embedding Ce/Tb: YAG crystals into a tapered optical fiber sensor. The breakthrough lies in the unique design of the tapered optical fiber, allowing efficient coupling of the scintillation light emitted by the Ce/Tb: YAG crystals into the tapered region, which is then conducted into the fused silica fiber. Through fusion splicing with multimode optical fibers, a response four times higher than traditional plastic scintillating fiber sensors was achieved. In 2022, Rajbhar et al. [135] successfully detected ions with energies as low as 80 keV using a tapered optical fiber. This achievement provides robust support for the development of portable devices for the detection of charged particles in nuclear reactors and even in space.

Although tapered optical fiber sensors hold potential in radiation dose measurement, their research has not been fully developed due to technical challenges such as accurately measuring high-dose radiation or dealing with proton irradiation. Through continuous innovation and optimization of designs, tapered optical fiber sensors are poised to become a key technology in the future of radiation dose measurement, providing precise and efficient solutions for nuclear safety and even aerospace applications.

3.3.2. Gas (Ammonia) Leak Detection

In industrial production, various harmful, combustible, or toxic gases may be involved. Timely detection of gas leaks can prevent accidents and ensure the safety of workers.

Tapered optical fibers have been extensively researched for their application in gas leak detection, enabling more sensitive detection.

Ammonia is involved in various industries such as agriculture, food processing, and chemical manufacturing, making the detection of ammonia leaks crucial for safety and quality control. Pakdeevanich [136] developed a simple responsive sensor for trace concentrations of ammonia gas using a tapered optical fiber, demonstrating better interactions compared to non-tapered optical fiber sensors. To determine the optimal geometric shape for gas leak detection, Riahi et al. [137] introduced a step-cascading approach to study the impact of geometric shapes on the gas detection performance of the sensor. With the rise of nanomaterials, Fan et al. [138] utilized a thick GO film, achieving a sensitivity of 4.97 pm/ppm within the range of 0–151 ppm ammonia concentration, as shown in Figure 25. However, the response time increased to 5 min, highlighting the need to address the time cost. Mohammed et al. [139] coated an etched tapered FBG with polyaniline/graphene nanofiber nanocomposites, enhancing the adsorption capacity for NH3 molecules and achieving high sensitivity and excellent selectivity for NH3 under room temperature conditions. As shown in Figure 26, during NH3 exposure, the change in the sensor's output optical power was significantly higher than the response to CH4, making this sensor practically valuable under room temperature conditions.

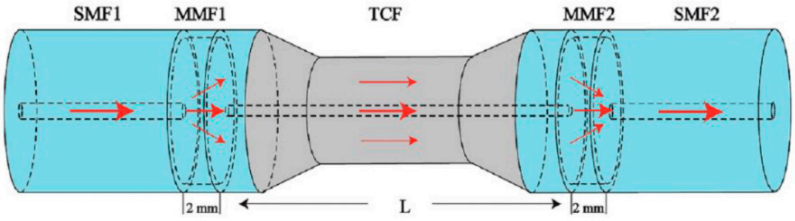

Figure 25. Schematic of the sensor designed by Fan et al. [138].

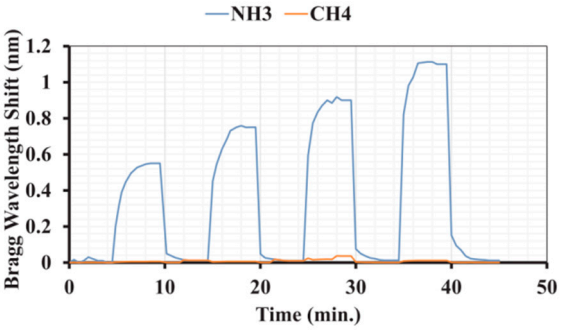

Figure 26. Dynamic response of the sensor at different ammonia and methane concentrations [139].

3.4. Summary

From the detection of biomolecular concentrations to temperature and humidity sensing, and further to ethanol concentration in water and ammonia gas leakage detection, the unique and excellent parameters and structural characteristics of tapered optical fiber sensors are evident in various fields. Table 2 summarizes the performance of tapered optical fiber sensors under different biochemical parameters. Taking BSA and Staphylococcus aureus as examples, variations in sensitivity, detection limits, and response times are demonstrated with different sizes and coatings. Cancer cell sensing exhibits high sensitivity to adrenal cancer. Additionally, for ammonia gas and ethanol, the flexibility in gas and liquid sensing is presented through the use of different coatings and sizes of tapered structures.

Table 2. Summary of biochemical parameters of tapered fiber optic sensors.

Analyte	Taper Length/ Waist Diameter	Sensitivity/Limit of Detection	Coating Material	Response/ Recovery Times	Ref
Bovine serum albumin (BSA)	Length 10 mm Waist 18.1 μm	LoD 125 pg/mL	BSA antigen	——	[99]
	Length 1 mm Waist 37 mm	0.0342/(mg/mL) LoD 0.971 μg/mL	Gold	Response 5 s	[140]
Staphylococcus aureus	Waist 10 μm	LoD 3.1 CFU/mL	porcine IgG antibody	Response <30 min	[112]
	Length 379 μm Waist 83.3 μm	2731.1 nm/RIU LoD 11 CFU/mL	Porcine IgG	Response <30 min	[114]
Cancer cell	——	adrenal cancer 15.2414 μm/RIU LoD 7.2 × 10^{-5} RIU	Graphene-Antimonene	——	[117]
	——	682.5 nm/RIU	——	——	[141]
Ethanol concentration (in water)	Waist 28 μm	14.9 (count/%)	ZnO	Response 0.6 s	[132]
	Waist 7 μm	0.886 nm/%	TiO2	——	[142]
Ammonia (gas)	Length 2 mm Waist 15 μm	0.72 nm/vol%	PANI \GNF Composite	Response 80 s recovery 36 s	[139]
	Length 30 mm Waist 80 μm	4.97 pm/ppm	GO	Response 5 min recovery 7.5 min	[138]

Table 3 summarizes the performance of tapered optical fiber sensors in temperature and humidity measurements. For temperature measurements, tapered structures of different sizes and designs exhibit varying sensitivities, suitable for different temperature ranges. In humidity measurements, by adjusting the size and structure, sensitivities within different dynamic ranges, ranging from 0.1194 nm/(%RH) to 59.8 pm/(%RH), are demonstrated. This indicates that tapered optical fiber sensors possess wide applicability and performance flexibility in temperature and humidity measurements.

Table 3. Summary of physical parameter measurements for tapered fiber optic sensors.

Measurand	Taper Length/ Waist Diameter	Sensitivity	Dynamic Range	Ref
Temperature	Length 2.5 mm Waist 4.9 μm	−415 pm/°C	30–50 °C	[143]
	Length 5 mm	−0.0393 nm/°C	30–90 °C	[144]
	Length 8 mm Waist 3 μm	−2.283 nm/°C	21.5–28 °C	[145]
	Length 370 μm Waist 90 μm	79.8 pm/°C	25–60 °C	[146]
Humidity	Waist 9 μm	0.1194 nm/%RH	30–90%RH	[147]
	Length 28 mm Waist 9.03 μm	0.5290 RH (%)	20–99.9%RH	[148]
	Length 1.3 mm Waist 7.82 μm	0.789 nm/%RH	70–89%RH	[149]
	Waist 8.52 μm	59.8 pm/(%RH)	35–95%RH	[150]

Different sensor applications focus on varying requirements, necessitating diverse fiber optic structures for implementation. Biomolecular concentration detection emphasizes low detection limits and high sensitivity, while temperature and humidity sensing pursues long-term stability, high sensitivity, and a broad range of temperature and humidity. Ethanol concentration detection aims for continuous improvement in response time and linearity. These diverse demands drive the continuous development of fiber optic sensor structures. We can anticipate the ongoing evolution of cone-shaped fiber optic technology, providing highly adaptive and excellent performance sensor solutions for various fields, such as food quality testing [151], detection of bridges, buildings, or other engineering structures [152–154], structural health monitoring in aerospace applications [155], and measurement of displacement [156].

4. Conclusions

Research on sensing based on fused tapered optical fibers continues to develop in both structural innovation and application expansion. Its advantages, including high sensitivity, real-time monitoring, immunity to electromagnetic interference, multi-parameter measurement capability, high resolution, and surface functionalization, have made it a research hotspot. This review systematically introduces common tapered optical fiber structures and discusses the applications of current popular sensors related to tapered optical fibers, including biosensing, environmental monitoring, and industrial monitoring.

Further exploration is needed in the fabrication of tapered structures on different optical fibers to overcome challenges such as limitations on sample size and shape, stability affected by the environment, and susceptibility to damage of the tapered tip. Reducing performance fluctuations caused by manufacturing process variations is crucial to ensure reliability and repeatability.

Overall, there is still significant research space for fused tapered optical fiber sensing to improve sensitivity, achieve miniaturization and integration, and explore cross-disciplinary developments with fields such as nanomaterials, quantum structures, and nanophotonics. The emergence of new materials like graphene oxide and carbon nanomaterials, coupled with ongoing technological advancements, will continue to drive the application of fused tapered optical fiber sensors in broader fields such as life sciences, photonics, and quantum technology, providing more possibilities for the development and innovation of sensing technology.

Author Contributions: S.B. wrote this manuscript; Y.L. proposed the idea and revised the manuscript. All authors have read and agreed to the published version of the manuscript.

Funding: This research was funded by the National Natural Science Foundation of China, grant No. 61905062 (Yudong Lian), and the China Postdoctoral Science Foundation, grant No. 2020M670613 (Yudong Lian).

Institutional Review Board Statement: Not applicable.

Informed Consent Statement: Not applicable.

Data Availability Statement: Not applicable.

Conflicts of Interest: The authors declare no conflicts of interest.

References

1. Birks, T.A.; Li, Y.W. The shape of fiber tapers. *J. Light. Technol.* **1992**, *10*, 432–438. [CrossRef]
2. Xiong, Y.; Xu, F. Multifunctional integration on optical fiber tips: Challenges and opportunities. *Adv. Photonics* **2020**, *2*, 064001. [CrossRef]
3. Li, G.; Liu, Z.; Feng, J.; Zhou, G.; Huang, X. Pb^{2+} fiber optic sensor based on smart hydrogel coated Mach–Zehnder interferometer. *Opt. Laser Technol.* **2022**, *145*, 107453. [CrossRef]
4. Liu, Y.; Lin, W.; Zhao, F.; Hu, J.; Chen, J.; Liu, H.; Shum, P.P.; Zhang, X.; Shao, L.-Y. Adaptive Fiber Ring Laser Based on Tapered Polarization Maintaining Fiber in Sagnac Loop for Temperature and Salinity Sensing. *Photonics* **2023**, *10*, 599. [CrossRef]

5. Kumari, A.; Vyas, V.; Kumar, S. Synthesis, characterization, and applications of gold nanoparticles in development of plasmonic optical fiber-based sensors. *Nanotechnology* **2022**, *34*, 042001. [CrossRef] [PubMed]
6. Zhou, H.; Suo, L.; Peng, Y.-P.; Yang, F.; Ren, S.; Chen, N.-K.; Lu, X.; Rahman, B.; Grattan, K. Micro-tapered fiber few-mode interferometers incorporated by molecule self-assembly fiber grating for temperature sensing applications. *Photonics* **2022**, *9*, 96. [CrossRef]
7. Zainuddin, N.H.; Chee, H.Y.; Rashid, S.A.; Ahmad, M.Z.; Zan, Z.; Bakar, M.H.A.; Alresheedi, M.T.; Mahdi, M.A.; Yaacob, M.H. Enhanced detection sensitivity of Leptospira DNA using a post-deposition annealed carbon quantum dots integrated tapered optical fiber biosensor. *Opt. Mater.* **2023**, *141*, 113926. [CrossRef]
8. Roriz, P.; Carvalho, L.; Frazão, O.; Santos, J.L.; Simões, J.A. From conventional sensors to fibre optic sensors for strain and force measurements in biomechanics applications: A review. *J. Biomech.* **2014**, *47*, 1251–1261. [CrossRef]
9. Golden, J.P.; Anderson, G.P.; Rabbany, S.; Ligler, F. An evanescent wave biosensor. II. Fluorescent signal acquisition from tapered fiber optic probes. *IEEE Trans. Biomed. Eng.* **1994**, *41*, 585–591. [CrossRef]
10. Correia, R.; James, S.; Lee, S.; Morgan, S.; Korposh, S. Biomedical application of optical fibre sensors. *J. Opt.* **2018**, *20*, 073003. [CrossRef]
11. Soria, S.; Berneschi, S.; Brenci, M.; Cosi, F.; Conti, G.N.; Pelli, S.; Righini, G.C. Optical microspherical resonators for biomedical sensing. *Sensors* **2011**, *11*, 785–805. [CrossRef] [PubMed]
12. Liu, H.; Miao, Y.; Liu, B.; Lin, W.; Zhang, H.; Song, B.; Huang, M.; Lin, L. Relative humidity sensor based on S-taper fiber coated with SiO 2 nanoparticles. *IEEE Sens. J.* **2015**, *15*, 3424–3428. [CrossRef]
13. Yu, Y.; Bian, Q.; Lu, Y.; Zhang, X.; Yang, J.; Liang, L. High sensitivity all optical fiber conductivity-temperature-depth (CTD) sensing based on an optical microfiber coupler (OMC). *J. Light. Technol.* **2018**, *37*, 2739–2747. [CrossRef]
14. Bariain, C.; Matías, I.R.; Arregui, F.J.; Lopez-Amo, M. Optical fiber humidity sensor based on a tapered fiber coated with agarose gel. *Sens. Actuators B Chem.* **2000**, *69*, 127–131. [CrossRef]
15. Zhang, W.; Zhuang, W.; Dong, M.; Zhu, L.; Meng, F. Dual-parameter optical fiber sensor for temperature and pressure discrimination featuring cascaded tapered-FBG and ball-EFPI. *IEEE Sens. J.* **2019**, *19*, 5645–5652. [CrossRef]
16. Kim, Y.-C.; Peng, W.; Banerji, S.; Booksh, K.S. Tapered fiber optic surface plasmon resonance sensor for analyses of vapor and liquid phases. *Opt. Lett.* **2005**, *30*, 2218–2220. [CrossRef]
17. Jin, B.; Wang, D. Multimode fiber surface plasmon resonance sensor based on a down–up taper. *Opt. Lett.* **2022**, *47*, 5329–5332. [CrossRef] [PubMed]
18. Sun, G.; Wu, G.; Wang, F.; Tang, R.; Qiu, G. High-stress resistance fiber refractometer based on MMF sandwiched between two SMF half-tapers. *IEEE Photonics Technol. Lett.* **2016**, *28*, 1336–1339. [CrossRef]
19. Fu, X.; Zhang, Y.; Zhou, J.; Li, Q.; Fu, G.; Jin, W.; Bi, W.; Hu, Q. A temperature and strain dual-parameter sensor based on conical four-core fiber combined with a multimode fiber. *IEEE Sens. J.* **2022**, *22*, 23990–23996. [CrossRef]
20. Shen, T.; Gong, A.; Chen, J.; Liu, C.; Liu, X.; Feng, Y.; Duan, S. An investigation on temperature sensor of SDTMS structure with Ag-ZnO/graphene cladding. *Opt. Laser Technol.* **2022**, *153*, 108275. [CrossRef]
21. Deng, L.; Jiang, C.; Hu, C.; Li, L.; Gao, J.; Li, H.; Sun, S.; Liu, C.; Shu, Y. Highly Sensitive Temperature and Gas Pressure Sensor Based on Long-Period Fiber Grating Inscribed in Tapered Two-Mode Fiber and PDMS. *IEEE Sens. J.* **2023**, *23*, 15578–15585. [CrossRef]
22. Liu, Y.; Xie, S.; Zheng, Y.; Yang, X. Simultaneous measurement of refractive index and temperature based on tapered no-core fiber cascaded with a fiber Bragg grating. *Results Opt.* **2022**, *9*, 100300. [CrossRef]
23. Zhu, C.; Huang, S.; Meng, X.; Zhao, Y.; Li, H. Deeply-Tapered Ultrashort Long-Period Fiber Grating and Its Application to Ultrasensitive Transverse-Load Sensor. *J. Light. Technol.* **2023**, *41*, 6108–6115. [CrossRef]
24. Kang, X.; Wang, R.; Jiang, M.; Li, E.; Li, Y.; Yan, X.; Wang, T.; Ren, Z. Polydopamine functionalized graphene oxide for high sensitivity micro-tapered long period fiber grating sensor and its application in detection Co_2^+ ions. *Opt. Fiber Technol.* **2022**, *68*, 102807. [CrossRef]
25. Fan, R.; Ma, Q.; Li, L.; Zhuo, Y.; Shen, J.; Ren, Z.; Chen, H.; Peng, B. Liquid level and refractive index double-parameter sensor based on tapered photonic crystal fiber. *J. Light. Technol.* **2020**, *38*, 3717–3722. [CrossRef]
26. Abbas, S.K.; Ahmed, S.S. Refractive index sensor based on tapered photonic crystal fiber to determine the performance of different carbonated liquids. *J. Opt.* **2023**. [CrossRef]
27. Gao, B.; Zhong, H.; Yan, B.; Yue, L.; Dang, Y.; Chen, P.; Jiang, C.; Wang, Z. Combined single/dual fiber optical trapping for flexible particle manipulation. *Opt. Lasers Eng.* **2023**, *161*, 107373. [CrossRef]
28. Deng, H.; Chen, D.; Wang, R.; Li, F.; Luo, Z.; Deng, S.; Yin, J.; Yu, L.; Zhang, W.; Yuan, L. Fiber-integrated optical tweezers for ballistic transport and trapping yeast cells. *Nanoscale* **2022**, *14*, 6941–6948. [CrossRef]
29. Li, X.; Chen, N.; Zhou, X.; Zhang, Y.; Zhao, Y.; Nguyen, L.V.; Ebendorff-Heidepriem, H.; Warren-Smith, S.C. In-situ DNA detection with an interferometric-type optical sensor based on tapered exposed core microstructured optical fiber. *Sens. Actuators B Chem.* **2022**, *351*, 130942. [CrossRef]
30. Zhao, F.; Lin, W.; Hu, J.; Liu, S.; Yu, F.; Chen, X.; Wang, G.; Shum, P.P.; Shao, L. Highly sensitive salinity and temperature measurement based on tapered-SHF MZI fiber laser structure. *Meas. Sci. Technol.* **2023**, *34*, 064002. [CrossRef]
31. Yang, J.; Lv, Y.; Li, P.; Zhang, G.; Lv, M.; Meng, L. Highly sensitive current sensor based on fiber loop Ring-Down spectroscopy and Bent-Annealed taper No-Core fiber surrounded by magnetic fluid. *Opt. Laser Technol.* **2023**, *162*, 109260. [CrossRef]

32. Bai, P.; Gao, Y.; Zhang, H.; Jin, B. A high-sensitivity magnetic field sensor using spindly optical fiber taper. *Opt. Fiber Technol.* **2023**, *78*, 103332. [CrossRef]
33. Zakariyah, S.S.; Conway, P.P.; Hutt, D.A.; Selviah, D.R.; Wang, K.; Baghsiahi, H.; Rygate, J.; Calver, J.; Kandulski, W. Polymer optical waveguide fabrication using laser ablation. In Proceedings of the 2009 11th Electronics Packaging Technology Conference, Singapore, 9–11 December 2009; pp. 936–941.
34. Xu, Y.; Geng, Y.; Wang, L.; Kumar, A.G.; Fang, L.; Du, Y.; Li, X. Femtosecond laser ablated pyramidal fiber taper-SERS probe with laser-induced silver nanostructures. *J. Phys. D Appl. Phys.* **2018**, *51*, 285104. [CrossRef]
35. Brambilla, G.; Xu, F.; Horak, P.; Jung, Y.; Koizumi, F.; Sessions, N.P.; Koukharenko, E.; Feng, X.; Murugan, G.S.; Wilkinson, J.S. Optical fiber nanowires and microwires: Fabrication and applications. *Adv. Opt. Photonics* **2009**, *1*, 107–161. [CrossRef]
36. Pang, S.; Shao, X.; Li, W.; Chen, X.; Gong, S. Dynamic characteristics and mechanisms of compressible metallic vapor plume behaviors in transient keyhole during deep penetration fiber laser welding. *Appl. Phys. A* **2016**, *122*, 702. [CrossRef]
37. Pricking, S.; Giessen, H. Tapering fibers with complex shape. *Opt. Express* **2010**, *18*, 3426–3437. [CrossRef]
38. Felipe, A.; Espíndola, G.; Kalinowski, H.J.; Lima, J.A.; Paterno, A.S. Stepwise fabrication of arbitrary fiber optic tapers. *Opt. Express* **2012**, *20*, 19893–19904. [CrossRef] [PubMed]
39. Harun, S.W.; Lim, K.; Tio, C.; Dimyati, K.; Ahmad, H. Theoretical analysis and fabrication of tapered fiber. *Optik* **2013**, *124*, 538–543. [CrossRef]
40. Korposh, S.; James, S.W.; Lee, S.-W.; Tatam, R.P. Tapered optical fibre sensors: Current trends and future perspectives. *Sensors* **2019**, *19*, 2294. [CrossRef]
41. Shabaneh, A.; Girei, S.; Arasu, P.; Rahman, W.; Bakar, A.; Sadek, A.; Lim, H.; Huang, N.; Yaacob, M. Reflectance response of tapered optical fiber coated with graphene oxide nanostructured thin film for aqueous ethanol sensing. *Opt. Commun.* **2014**, *331*, 320–324. [CrossRef]
42. Ibrahim, S.; Rahman, N.; Bakar, M.A.; Girei, S.; Yaacob, M.; Ahmad, H.; Mahdi, M. Room temperature ammonia sensing using tapered multimode fiber coated with polyaniline nanofibers. *Opt. Express* **2015**, *23*, 2837–2845. [CrossRef] [PubMed]
43. Qiu, H.; Gao, S.; Chen, P.; Li, Z.; Liu, X.; Zhang, C.; Xu, Y.; Jiang, S.; Yang, C.; Huo, Y. Evanescent wave absorption sensor based on tapered multimode fiber coated with monolayer graphene film. *Opt. Commun.* **2016**, *366*, 275–281. [CrossRef]
44. Chauhan, M.; Singh, V.K. Tapered MMF sensor fabrication using SnO2-NPs for alcohol sensing application. *Opt. Fiber Technol.* **2023**, *75*, 103167. [CrossRef]
45. Gao, R.; Wang, H.; Zhu, D.; Fan, G.; Yan, H.; Wang, P.; Liu, Y.; Wang, Y.; Liu, W.; Song, L. Acoustic frequency vibration sensor based on tapered SMS fiber structure. *Sens. Actuators A Phys.* **2018**, *271*, 243–250. [CrossRef]
46. Wang, P.; Brambilla, G.; Ding, M.; Semenova, Y.; Wu, Q.; Farrell, G. High-sensitivity, evanescent field refractometric sensor based on a tapered, multimode fiber interference. *Opt. Lett.* **2011**, *36*, 2233–2235. [CrossRef]
47. André, R.M.; Biazoli, C.R.; Silva, S.O.; Marques, M.B.; Cordeiro, C.M.; Frazão, O. Multimode interference in tapered single mode-multimode-single mode fiber structures for strain sensing applications. In Proceedings of the OFS2012 22nd International Conference on Optical Fiber Sensors, Beijing, China, 15–19 October 2012; pp. 576–579.
48. Zhao, Y.; Cai, L.; Hu, H.-F. Fiber-optic refractive index sensor based on multi-tapered SMS fiber structure. *IEEE Sens. J.* **2015**, *15*, 6348–6353. [CrossRef]
49. Yang, B.; Niu, Y.; Yang, B.; Hu, Y.; Dai, L.; Yin, Y.; Ding, M. High sensitivity balloon-like refractometric sensor based on singlemode-tapered multimode-singlemode fiber. *Sens. Actuators A Phys.* **2018**, *281*, 42–47. [CrossRef]
50. Song, D.; Chai, Q.; Liu, Y.; Jiang, Y.; Zhang, J.; Sun, W.; Yuan, L.; Canning, J.; Peng, G.-D. A simultaneous strain and temperature sensing module based on FBG-in-SMS. *Meas. Sci. Technol.* **2014**, *25*, 055205. [CrossRef]
51. Wang, J.; Wang, L.; Su, X.; Xiao, R.; Cheng, H. Temperature, stress, refractive index and humidity multi parameter highly integrated optical fiber sensor. *Opt. Laser Technol.* **2022**, *152*, 108086. [CrossRef]
52. Tian, K.; Xin, Y.; Yang, W.; Geng, T.; Ren, J.; Fan, Y.-X.; Farrell, G.; Lewis, E.; Wang, P. A curvature sensor based on twisted single-mode–multimode–single-mode hybrid optical fiber structure. *J. Light. Technol.* **2017**, *35*, 1725–1731. [CrossRef]
53. Li, S.; Nezami, M.S.; Mishra, S.; Liboiron-Ladouceur, O. Spectral-dependent electronic-photonic modeling of high-speed VCSEL-MMF links for optimized launch conditions. *Opt. Express* **2021**, *29*, 2738–2756. [CrossRef]
54. Yang, Q.; Hu, D.; Li, Z.; Xu, Z.; Ran, Y.; Guan, B.-o. Assembly tapered fiber Bragg grating tip with gold nanostars for heat generation and gradient temperature sensing. *Opt. Laser Technol.* **2024**, *175*, 110759. [CrossRef]
55. Zhao, X.; Zhang, Y.; Zhang, W.; Li, Z.; Kong, L.; Yu, L.; Ge, J.; Yan, T. Ultra-high sensitivity and temperature-compensated Fabry–Perot strain sensor based on tapered FBG. *Opt. Laser Technol.* **2020**, *124*, 105997. [CrossRef]
56. Li, P.; Yan, H.; Xie, Z.; Li, Y.; Zhao, X. An intensity-modulated and large bandwidth magnetic field sensor based on a tapered fiber Bragg grating. *Opt. Laser Technol.* **2020**, *125*, 105996. [CrossRef]
57. Mishra, V.; Singh, N.; Tiwari, U.; Kapur, P. Fiber grating sensors in medicine: Current and emerging applications. *Sens. Actuators A Phys.* **2011**, *167*, 279–290. [CrossRef]
58. Bock, W.J.; Chen, J.; Mikulic, P.; Eftimov, T. A novel fiber-optic tapered long-period grating sensor for pressure monitoring. *IEEE Trans. Instrum. Meas.* **2007**, *56*, 1176–1180. [CrossRef]
59. Lee, C.-L.; Weng, Z.-Y.; Lin, C.-J.; Lin, Y. Leakage coupling of ultrasensitive periodical silica thin-film long-period grating coated on tapered fiber. *Opt. Lett.* **2010**, *35*, 4172–4174. [CrossRef] [PubMed]

60. Shao, F.; Li, S.; Lu, L.; Kuai, Y.; Cao, Z.; Xu, F.; Liu, Y.; Xie, F.; Xie, K.; Yu, B. High sensitivity and dual parameters micro-tapered-LPG sensor. *Opt. Lasers Eng.* **2023**, *164*, 107498. [CrossRef]
61. Lee, S.-L.; Kim, J.; Choi, S.; Han, J.; Seo, G.; Lee, Y.W. Fiber-optic label-free biosensor for SARS-CoV-2 spike protein detection using biofunctionalized long-period fiber grating. *Talanta* **2021**, *235*, 122801. [CrossRef]
62. Dudley, J.M.; Taylor, J.R. Ten years of nonlinear optics in photonic crystal fibre. *Nat. Photonics* **2009**, *3*, 85–90. [CrossRef]
63. Frazao, O.; Santos, J.L.; Araujo, F.M.; Ferreira, L.A. Optical sensing with photonic crystal fibers. *Laser Photonics Rev.* **2008**, *2*, 449–459. [CrossRef]
64. Wang, H.; Tong, K.; Cui, W.; Li, Z. Study of temperature measurement with one-dimensional photonic crystal. In Proceedings of the Lasers in Material Processing and Manufacturing III, Beijing, China, 11–15 November 2007; pp. 348–353.
65. Zhao, Y.; Li, X.-G.; Cai, L.; Yang, Y. Refractive index sensing based on photonic crystal fiber interferometer structure with up-tapered joints. *Sens. Actuators B Chem.* **2015**, *221*, 406–410. [CrossRef]
66. Fan, R.; Li, L.; Zhuo, Y.; Lv, X.; Ren, Z.; Shen, J.; Peng, B. Practical research on photonic crystal fiber micro-strain sensor. *Opt. Fiber Technol.* **2019**, *52*, 101959. [CrossRef]
67. Dass, S.; Dash, J.N.; Jha, R. Intensity modulated SMF cascaded tapers with a hollow core PCF based microcavity for curvature sensing. *J. Opt.* **2016**, *18*, 035006. [CrossRef]
68. Tu, T.; Pang, F.; Zhu, S.; Cheng, J.; Liu, H.; Wen, J.; Wang, T. Excitation of Bloch surface wave on tapered fiber coated with one-dimensional photonic crystal for refractive index sensing. *Opt. Express* **2017**, *25*, 9019–9027. [CrossRef]
69. Li, X.; Yu, Q.; Zhou, X.; Zhang, Y.; Lv, R.; Zhao, Y. Magnetic sensing technology of fiber optic interferometer based on magnetic fluid: A review. *Measurement* **2023**, *216*, 112929. [CrossRef]
70. Benazza, A.; Beffara, F.; Auguste, J.-L.; Olivo, M.; Dinish, U.; Humbert, G. Reliable and easy-to-use SERS spectroscopy probe using a tapered opto-fluidic photonic crystal fiber. *Opt. Express* **2024**, *32*, 3440–3450. [CrossRef] [PubMed]
71. Zhao, X.; Zhao, N.; Shi, Y.; Xin, H.; Li, B. Optical fiber tweezers: A versatile tool for optical trapping and manipulation. *Micromachines* **2020**, *11*, 114. [CrossRef]
72. Taha, B.A.; Ali, N.; Sapiee, N.M.; Fadhel, M.M.; Mat Yeh, R.M.; Bachok, N.N.; Al Mashhadany, Y.; Arsad, N. Comprehensive review tapered optical fiber configurations for sensing application: Trend and challenges. *Biosensors* **2021**, *11*, 253. [CrossRef]
73. Huang, J.; Liu, X.; Zhang, Y.; Li, B. Optical trapping and orientation of Escherichia coli cells using two tapered fiber probes. *Photonics Res.* **2015**, *3*, 308–312. [CrossRef]
74. Liu, Z.; Wang, T.; Zhang, Y.; Tang, X.; Liu, P.; Zhang, Y.; Yang, X.; Zhang, J.; Yang, J.; Yuan, L. Single fiber dual-functionality optical tweezers based on graded-index multimode fiber. *Chin. Opt. Lett.* **2018**, *16*, 053501.
75. Wang, T.; Jiang, J.; Liu, K.; Wang, S.; Zhang, Y.; Niu, P.; Liu, T. Pendulum-style adjustment of captured particles with fiber tweezers based on asymmetrical fiber tip for CARS system. In Proceedings of the Advanced Sensor Systems and Applications X, Online, 11–16 October 2020; pp. 24–29.
76. Rong, Q.; Wang, Y.; Shao, Z.; Qiao, X. Large diameter fiber-optics tweezers for escherichia coli bacteria manipulation. *IEEE J. Sel. Top. Quantum Electron.* **2018**, *25*, 1–7. [CrossRef]
77. Asadollahbaik, A.; Thiele, S.; Weber, K.; Kumar, A.; Drozella, J.; Sterl, F.; Herkommer, A.M.; Giessen, H.; Fick, J. Highly efficient dual-fiber optical trapping with 3D printed diffractive fresnel lenses. *Acs Photonics* **2019**, *7*, 88–97. [CrossRef]
78. Fooladi, E.; Sadeghi, M.; Adelpour, Z.; Bahadori-Jahromi, F. Performance improvement of a plasmonic tapered twin–core fiber optical tweezers. *Optik* **2021**, *245*, 167656. [CrossRef]
79. Novotny, L.; Bian, R.X.; Xie, X.S. Theory of nanometric optical tweezers. *Phys. Rev. Lett.* **1997**, *79*, 645. [CrossRef]
80. Kaya, M.; Sahay, P.; Wang, C. Reproducibly reversible fiber loop ringdown water sensor embedded in concrete and grout for water monitoring. *Sens. Actuators B Chem.* **2013**, *176*, 803–810. [CrossRef]
81. Wang, C. Fiber loop ringdown—A time-domain sensing technique for multi-function fiber optic sensor platforms: Current status and design perspectives. *Sensors* **2009**, *9*, 7595–7621. [CrossRef] [PubMed]
82. Yu, D.; Humar, M.; Meserve, K.; Bailey, R.C.; Chormaic, S.N.; Vollmer, F. Whispering-gallery-mode sensors for biological and physical sensing. *Nat. Rev. Methods Primers* **2021**, *1*, 83. [CrossRef]
83. Li, X.; Wang, X.; Niu, P.; Zhao, J.; Zhang, C.; Gu, E. Refractive index measurement using OTDR-based ring-down technique with S fiber taper. *Opt. Commun.* **2019**, *446*, 186–190. [CrossRef]
84. Tian, J.; Yang, L.; Qin, C.; Wu, T.; Wang, J.; Zhang, Z.; Li, K.; Copner, N.J. Refractive index sensing based on chaotic correlation fiber loop ring down system using tapered fiber. *IEEE Sens. J.* **2019**, *20*, 4215–4220. [CrossRef]
85. Wang, F.; Li, H.; Wang, X.; Ma, T.; Yu, K.; Lu, Y.; Zhang, L.; Liu, Y. Temperature and curvature measurement based on low cavity loss FLRD technology. *IEEE Sens. J.* **2021**, *22*, 2221–2228. [CrossRef]
86. Cheng, C.; Chen, J.; Chen, Z.; Ou, Y. Large-dynamic-range fiber loop ringdown strain sensor using Frequency-shifted Interferometry. *Opt. Quantum Electron.* **2021**, *53*, 318. [CrossRef]
87. Chen, Z.; Cheng, C.; Ou, Y.; Yang, Z.; Chen, J.; Lv, H. Multipoint strain sensing system based on fiber loop ringdown and frequency-shifted interferometry. In Proceedings of the AOPC 2019: Optical Sensing and Imaging Technology, Beijing, China, 7–9 July 2019; pp. 177–182.
88. Jiang, Q.; Yang, L.; Guo, Y.; Wang, J.; Xue, P.; Liu, J. Multi-channel chaotic cross-correlation fiber loop ring down sensing. *Opt. Commun.* **2023**, *540*, 129502. [CrossRef]
89. Lechuga, L.M. Optical biosensors. *Compr. Anal. Chem.* **2005**, *44*, 209–250.

90. Wang, Q.; Kong, L.; Dang, Y.; Xia, F.; Zhang, Y.; Zhao, Y.; Hu, H.; Li, J. High sensitivity refractive index sensor based on splicing points tapered SMF-PCF-SMF structure Mach–Zehnder mode interferometer. *Sens. Actuators B Chem.* **2016**, *225*, 213–220. [CrossRef]
91. Pawar, D.; Kale, S. Birefringence manipulation in tapered polarization-maintaining photonic crystal fiber Mach–Zehnder interferometer for refractive index sensing. *Sens. Actuators A Phys.* **2016**, *252*, 180–184. [CrossRef]
92. Yang, J.; Jiang, L.; Wang, S.; Li, B.; Wang, M.; Xiao, H.; Lu, Y.; Tsai, H. High sensitivity of taper-based Mach–Zehnder interferometer embedded in a thinned optical fiber for refractive index sensing. *Appl. Opt.* **2011**, *50*, 5503–5507. [CrossRef] [PubMed]
93. Wang, F.; Pang, K.; Ma, T.; Wang, X.; Liu, Y. Folded-tapered multimode-no-core fiber sensor for simultaneous measurement of refractive index and temperature. *Opt. Laser Technol.* **2020**, *130*, 106333. [CrossRef]
94. Su, H.; Zhang, Y.; Ma, K.; Yi, G.; Zhao, Y.; Yu, C. Slight-offset tapered multimode fiber with high sensitivity for low refractive index range. *IEEE Sens. J.* **2020**, *20*, 9849–9855. [CrossRef]
95. Hu, H.; Song, X.; Han, Q.; Chang, P.; Zhang, J.; Liu, K.; Du, Y.; Wang, H.; Liu, T. High sensitivity fiber optic SPR refractive index sensor based on multimode-no-core-multimode structure. *IEEE Sens. J.* **2019**, *20*, 2967–2975. [CrossRef]
96. Ayupova, T.; Shaimerdenova, M.; Tosi, D. Shallow-tapered chirped fiber Bragg grating sensors for dual refractive index and temperature sensing. *Sensors* **2021**, *21*, 3635. [CrossRef]
97. Jin, X.; Sun, C.; Duan, S.; Liu, W.; Li, G.; Zhang, S.; Chen, X.; Zhao, L.; Lu, C.; Yang, X. High strain sensitivity temperature sensor based on a secondary modulated tapered long period fiber grating. *IEEE Photonics J.* **2019**, *11*, 1–8. [CrossRef]
98. Song, B.; Jin, C.; Wang, B.; Wu, J.; Liu, B.; Lin, W.; Huang, W.; Duan, S.; Qiao, M. Hydrophobin HGFI assisted immunobiologic sensor based on a cascaded taper integrated ultra-long-period fiber grating. *Biomed. Opt. Express* **2021**, *12*, 2790–2799. [CrossRef] [PubMed]
99. Minkovich, V.P.; Sotsky, A.B. Tapered photonic crystal fibers coated with ultra-thin films for highly sensitive bio-chemical sensing. *J. Eur. Opt. Soc. -Rapid Publ.* **2019**, *15*, 7. [CrossRef]
100. Wu, Y.; Liu, B.; Wang, J.; Wu, J.; Mao, Y.; Ren, J.; Zhao, L.; Sun, T.; Nan, T.; Han, Y. A novel temperature insensitive refractive index sensor based on dual photonic crystal fiber. *Optik* **2021**, *226*, 165495. [CrossRef]
101. Chen, W.W.; Zhao, C.L.; Wang, Z.K.; Mao, B.N. Curvature sensor based on SMF taper in fiber loop ring down system. *Opt. Fiber Technol.* **2019**, *52*, 101977. [CrossRef]
102. Ma, J.; Wu, S.; Cheng, H.; Yang, X.; Wang, S.; Lu, P. Sensitivity-enhanced temperature sensor based on encapsulated S-taper fiber Modal interferometer. *Opt. Laser Technol.* **2021**, *139*, 106933. [CrossRef]
103. Mumtaz, F.; Cheng, P.; Li, C.; Cheng, S.; Du, C.; Yang, M.; Dai, Y.; Hu, W. A design of taper-like etched multicore fiber refractive index-insensitive a temperature highly sensitive Mach–Zehnder interferometer. *IEEE Sens. J.* **2020**, *20*, 7074–7081. [CrossRef]
104. Liao, Y.-C.; Liu, B.; Liu, J.; Wan, S.-P.; He, X.-D.; Yuan, J.; Fan, X.; Wu, Q. High temperature (Up to 950 °C) sensor based on micro taper in-line fiber Mach–Zehnder interferometer. *Appl. Sci.* **2019**, *9*, 2394. [CrossRef]
105. Ahsani, V.; Ahmed, F.; Jun, M.B.; Bradley, C. Tapered fiber-optic Mach–Zehnder interferometer for ultra-high sensitivity measurement of refractive index. *Sensors* **2019**, *19*, 1652. [CrossRef]
106. Verma, R.K.; Sharma, A.K.; Gupta, B. Surface plasmon resonance based tapered fiber optic sensor with different taper profiles. *Opt. Commun.* **2008**, *281*, 1486–1491. [CrossRef]
107. Stokes, D.L.; Chi, Z.; Vo-Dinh, T. Surface-enhanced-Raman-scattering-inducing nanoprobe for spectrochemical analysis. *Appl. Spectrosc.* **2004**, *58*, 292–298. [CrossRef]
108. Zheng, D.; Wang, M.; Wang, M.; Zhai, M.; Wang, W. Measurement of droplet size and velocity based on a single tapered fiber optical reflectometer. *Measurement* **2022**, *189*, 110487. [CrossRef]
109. Ogert, R.A.; Brown, J.E.; Singh, B.R.; Shriver-Lake, L.C.; Ligler, F.S. Detection of Clostridium botulinum toxin A using a fiber optic-based biosensor. *Anal. Biochem.* **1992**, *205*, 306–312. [CrossRef] [PubMed]
110. Duan, S.; Wang, B.; Qiao, M.; Zhang, X.; Liu, B.; Zhang, H.; Song, B.; Wu, J. Hydrophobin HGFI–based fibre-optic biosensor for detection of antigen–antibody interaction. *Nanophotonics* **2019**, *9*, 177–186. [CrossRef]
111. Chen, X.; Xiao, L.; Li, X.; Yi, D.; Zhang, J.; Yuan, H.; Ning, Z.; Hong, X.; Chen, Y. Tapered Fiber Bioprobe Based on U-Shaped Fiber Transmission for Immunoassay. *Biosensors* **2023**, *13*, 940. [CrossRef] [PubMed]
112. Chen, L.; Leng, Y.-K.; Liu, B.; Liu, J.; Wan, S.-P.; Wu, T.; Yuan, J.; Shao, L.; Gu, G.; Fu, Y.Q. Ultrahigh-sensitivity label-free optical fiber biosensor based on a tapered singlemode-no core-singlemode coupler for Staphylococcus aureus detection. *Sens. Actuators B Chem.* **2020**, *320*, 128283. [CrossRef]
113. Cui, J.; Zhou, M.; Li, Y.; Liang, Z.; Li, Y.; Yu, L.; Liu, Y.; Liang, Y.; Chen, L.; Yang, C. A new optical fiber probe-based quantum dots immunofluorescence biosensors in the detection of Staphylococcus aureus. *Front. Cell. Infect. Microbiol.* **2021**, *11*, 665241. [CrossRef]
114. Li, H.-C.; Leng, Y.-K.; Liao, Y.-C.; Liu, B.; Luo, W.; Liu, J.; Shi, J.-L.; Yuan, J.; Xu, H.-Y.; Xiong, Y.-H. Tapered microfiber MZI Biosensor for highly sensitive detection of Staphylococcus aureus. *IEEE Sens. J.* **2022**, *22*, 5531–5539. [CrossRef]
115. Gupta, B.D. *Fiber Optic Sensors: Principles and Applications*; New India Publishing: New Delhi, India, 2006.
116. Liu, X.; Yuan, J.; Wu, D.; Zou, X.; Zheng, Q.; Zhang, W.; Lei, H. All-optical targeted drug delivery and real-time detection of a single cancer cell. *Nanophotonics* **2019**, *9*, 611–622. [CrossRef]
117. Vikas; Saccomandi, P. Antimonene-Coated Uniform-Waist Tapered Fiber Optic Surface Plasmon Resonance Biosensor for the Detection of Cancerous Cells: Design and Optimization. *ACS Omega* **2023**, *8*, 4627–4638. [CrossRef] [PubMed]

118. Pan, J.; Sun, X.; Feng, J.; Zeng, H. Tapered Fiber Based Infrared DNA Molecule Sensor. In Proceedings of the 2019 IEEE 4th Optoelectronics Global Conference (OGC), Shenzhen, China, 3–6 September 2019; pp. 81–84.
119. Sun, D.; Guo, T.; Ran, Y.; Huang, Y.; Guan, B.-O. In-situ DNA hybridization detection with a reflective microfiber grating biosensor. *Biosens. Bioelectron.* **2014**, *61*, 541–546. [CrossRef] [PubMed]
120. Song, B.; Zhang, H.; Liu, B.; Lin, W.; Wu, J. Label-free in-situ real-time DNA hybridization kinetics detection employing microfiber-assisted Mach–Zehnder interferometer. *Biosens. Bioelectron.* **2016**, *81*, 151–158. [CrossRef]
121. Zainuddin, N.H.; Chee, H.Y.; Ahmad, M.Z.; Mahdi, M.A.; Abu Bakar, M.H.; Yaacob, M.H. Sensitive Leptospira DNA detection using tapered optical fiber sensor. *J. Biophotonics* **2018**, *11*, e201700363. [CrossRef] [PubMed]
122. Zhang, X.; Liu, B.; Zhang, H.; Song, B.; Wu, J.; Duan, S. Label-free detection of DNA hybridization utilizing dual S-tapered thin-core fiber interferometer. *J. Light. Technol.* **2019**, *37*, 2762–2767. [CrossRef]
123. Zainuddin, N.H.; Chee, H.Y.; Rashid, S.A.; Ahmad, M.Z.; Bakar, M.H.A.; Mahdi, M.A.; Yaacob, M.H. Carbon quantum dots functionalized tapered optical fiber for highly sensitive and specific detection of Leptospira DNA. *Opt. Laser Technol.* **2023**, *157*, 108696. [CrossRef]
124. Bariain, C.; Matias, I.R.; Arregui, F.J.; Lopez-Amo, M. Experimental results toward development of humidity sensors by using a hygroscopic material on biconically tapered optical fiber. In Proceedings of the Optical and Fiber Optic Sensor Systems, Beijing, China, 16–19 September 1998; pp. 95–105.
125. Li, L.; Wang, Z.; Ma, Q.; Wang, M.; Wu, Q.; Chen, H.; Peng, B. Sagnac ring humidity sensor with a melting cone based on graphene properties. *IEEE Sens. J.* **2021**, *21*, 16061–16065. [CrossRef]
126. Quiñones-Flores, A.A.; Guzman-Sepulveda, J.R.; Castillo-Guzman, A.A. Relative Humidity Measurement Based on a Tapered, PVA-Coated Fiber Optics Multimode Interference Sensor. *Optics* **2023**, *4*, 473–481. [CrossRef]
127. Le, D.D.A.; Yoo, K.-W.; Lee, S.M.; Chung, H.; Cha, K.J.; Han, Y.-G. Few-mode microfiber knot resonator for measurement of relative humidity by considering group index difference (Conference Presentation). In Proceedings of the Optical Components and Materials XV, San Francisco, CA, USA, 27 January–1 February 2018; p. 105280I.
128. Kou, J.-l.; Feng, J.; Ye, L.; Xu, F.; Lu, Y.-q. Miniaturized fiber taper reflective interferometer for high temperature measurement. *Opt. Express* **2010**, *18*, 14245–14250. [CrossRef]
129. Tong, R.-j.; Zhao, Y.; Chen, M.-q.; Hu, X.-g.; Yang, Y. Simultaneous measurement of RH and temperature based on FBG and balloon-like sensing structure with inner embedded up-tapered MZI. *Measurement* **2019**, *146*, 1–8. [CrossRef]
130. Yang, H.-Z.; Qiao, X.-G.; Ali, M.M.; Islam, M.R.; Lim, K.-S. Optimized Tapered Optical Fiber for Ethanol (C_2H_5OH) Concentration Sensing. *J. Light. Technol.* **2014**, *32*, 1777–1783. [CrossRef]
131. Semwal, V.; Gupta, B. Localized Surface Plasmon Resonance Based Tapered Fiber Optic Ethanol Sensor. In Proceedings of the The European Conference on Lasers and Electro-Optics, Munich Germany, 23–27 June 2019; p. ch_p_10.
132. Azad, S.; Parvizi, R.; Sadeghi, E. Tapered optical fiber coated with ZnO nanorods for detection of ethanol concentration in water. *Int. J. Opt. Photonics* **2018**, *12*, 109–118. [CrossRef]
133. Khalaf, A.L.; Shabaneh, A.A.A.; Yaacob, M.H. Carbon Nanotubes and Graphene Oxide Applications in Optochemical Sensors. In *Synthesis, Technology and Applications of Carbon Nanomaterials*; Elsevier: Amsterdam, The Netherlands, 2019; pp. 223–246.
134. Jia, M.; Wen, J.; Pan, X.; Xin, Z.; Pang, F.; He, L.; Wang, T. Tapered fiber radiation sensor based on Ce/Tb: YAG crystals for remote γ-ray dosimetry. *Opt. Express* **2021**, *29*, 1210–1220. [CrossRef]
135. Rajbhar, M.K.; Maharana, B.; Patra, S.; Chatterjee, S. Tapered Optical Fiber-based Detection of Charged Particle Irradiation in Space Exploration and Nuclear Reactors. *arXiv* **2022**, arXiv:2210.13226.
136. Pakdeevanich, P. Tapered optical fiber ammonia sensor coated with phenol red and tetraethyl ortho silicate (TEOS). In Proceedings of the 2017 2nd International Conference on Frontiers of Sensors Technologies (ICFST), Shenzhen, China, 14–16 April 2017; pp. 78–81.
137. Riahi, A.; Vahedi, M.; Khalilzadeh, J.; Dastjerdi, V. Investigation of the effect of the taper geometry on the sensitivity of tapered-fibre gas sensors. *J. Mod. Opt.* **2020**, *67*, 1259–1266. [CrossRef]
138. Fan, X.; Deng, S.; Wei, Z.; Wang, F.; Tan, C.; Meng, H. Ammonia gas sensor based on graphene oxide-coated Mach–Zehnder interferometer with hybrid fiber structure. *Sensors* **2021**, *21*, 3886. [CrossRef]
139. Mohammed, H.; Yaacob, M. A novel modified fiber Bragg grating (FBG) based ammonia sensor coated with polyaniline/graphite nanofibers nanocomposites. *Opt. Fiber Technol.* **2020**, *58*, 102282. [CrossRef]
140. Peng, Y.; Zhao, Y.; Hu, X.-g.; Yang, Y. Optical fiber quantum biosensor based on surface plasmon polaritons for the label-free measurement of protein. *Sens. Actuators B Chem.* **2020**, *316*, 128097. [CrossRef]
141. Maiti, S.; Prakash, S.; Singh, V. Enhanced sensing performance of tapered profile in the apodized fiber Bragg grating for detection of cancerous cells utilizing their refractive index. *J. Biophotonics* **2023**, *16*, e202300237. [CrossRef]
142. Chauhan, M.; Singh, V.K. TiO_2 coated tapered optical fiber SPR sensor for alcohol sensing application. *J. Opt.* **2023**, *52*, 2285–2295. [CrossRef]
143. Wang, S.; Miao, Y.; Fei, C.; Zhang, H.; Li, B. A high-sensitivity temperature sensor based on a liquid cladding tapered microfiber. *IEEE Sens. J.* **2020**, *21*, 6152–6157. [CrossRef]
144. Fu, X.; Zhang, Y.; Wang, Y.; Fu, G.; Jin, W.; Bi, W. A temperature sensor based on tapered few mode fiber long-period grating induced by CO2 laser and fusion tapering. *Opt. Laser Technol.* **2020**, *121*, 105825. [CrossRef]

145. Lu, J.; Yu, Y.; Qin, S.; Li, M.; Bian, Q.; Lu, Y.; Hu, X.; Yang, J.; Meng, Z.; Zhang, Z. High-performance temperature and pressure dual-parameter sensor based on a polymer-coated tapered optical fiber. *Opt. Express* **2022**, *30*, 9714–9726. [CrossRef] [PubMed]
146. Wang, F.; Zhang, L.; Ma, T.; Wang, X.; Yu, K.; Liu, Y. A high-sensitivity sensor based on tapered dispersion compensation fiber for curvature and temperature measurement. *Opt. Commun.* **2021**, *481*, 126534. [CrossRef]
147. Chen, N.; Zhou, X.; Li, X. Highly sensitive humidity sensor with low-temperature cross-sensitivity based on a polyvinyl alcohol coating tapered fiber. *IEEE Trans. Instrum. Meas.* **2020**, *70*, 1–8. [CrossRef]
148. Syuhada, A.; Shamsudin, M.S.; Daud, S.; Krishnan, G.; Harun, S.W.; Aziz, M.S.A. Single-mode modified tapered fiber structure functionalized with GO-PVA composite layer for relative humidity sensing. *Photonic Sens.* **2021**, *11*, 314–324. [CrossRef]
149. Liu, Z.; Zhang, M.; Zhang, Y.; Xu, Y.; Zhang, Y.; Yang, X.; Zhang, J.; Yang, J.; Yuan, L. Spider silk-based tapered optical fiber for humidity sensing based on multimode interference. *Sens. Actuators A Phys.* **2020**, *313*, 112179. [CrossRef]
150. Cheng, J. In-fiber Mach–Zehnder interferometer based on multi-core microfiber for humidity and temperature sensing. *Appl. Opt.* **2020**, *59*, 756–763. [CrossRef] [PubMed]
151. Arjmand, M.; Saghafifar, H.; Alijanianzadeh, M.; Soltanolkotabi, M. A sensitive tapered-fiber optic biosensor for the label-free detection of organophosphate pesticides. *Sens. Actuators B Chem.* **2017**, *249*, 523–532. [CrossRef]
152. López-Higuera, J.M.; Cobo, L.R.; Incera, A.Q.; Cobo, A. Fiber optic sensors in structural health monitoring. *J. Light. Technol.* **2011**, *29*, 587–608. [CrossRef]
153. Kuang, K.S.; Cantwell, W.J.; Scully, P.J. An evaluation of a novel plastic optical fibre sensor for axial strain and bend measurements. *Meas. Sci. Technol.* **2002**, *13*, 1523. [CrossRef]
154. Willberry, J.O.; Papaelias, M.; Franklyn Fernando, G. Structural health monitoring using fibre optic acoustic emission sensors. *Sensors* **2020**, *20*, 6369. [CrossRef] [PubMed]
155. Di Sante, R. Fibre optic sensors for structural health monitoring of aircraft composite structures: Recent advances and applications. *Sensors* **2015**, *15*, 18666–18713. [CrossRef] [PubMed]
156. Binu, S.; Pillai, V.M.; Chandrasekaran, N. Fibre optic displacement sensor for the measurement of amplitude and frequency of vibration. *Opt. Laser Technol.* **2007**, *39*, 1537–1543. [CrossRef]